

UNIVERSITY OF NAPLES FEDERICO II

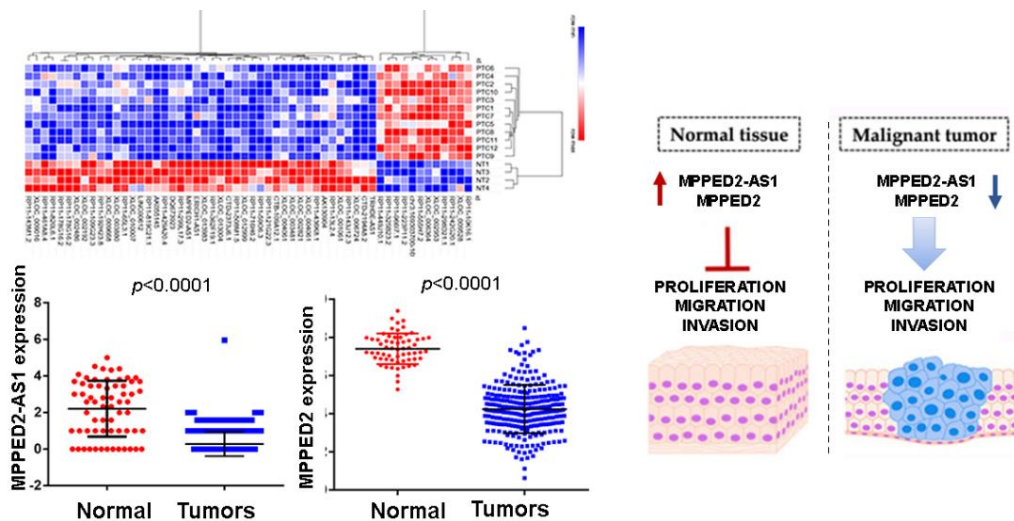
DOCTORATE IN
MOLECULAR MEDICINE AND MEDICAL BIOTECHNOLOGY

XXXII CYCLE



Simona Pellecchia

Role of *MPPED2-AS1* lncRNA and its associated-gene *MPPED2* in
thyroid and breast cancer



YEAR 2020

UNIVERSITY OF NAPLES FEDERICO II

**DOCTORATE IN
MOLECULAR MEDICINE AND MEDICAL BIOTECHNOLOGY**

XXXII CYCLE



**Role of *MPPED2-AS1* lncRNA and its associated-gene *MPPED2* in
thyroid and breast cancer**

**TUTOR
Prof. ALFREDO FUSCO**

**CANDIDATE
Dr. SIMONA PELLECCIA**

**COORDINATOR
Prof. VITTORIO ENRICO AVVEDIMENTO**

YEAR 2020

Index

Abstract.....	4
1. Background	5
1.1 Class of non-coding RNAs (ncRNAs)	5
1.2 Characteristics of lncRNAs.....	6
1.3 Molecular mechanisms of lncRNAs action	8
1.4 Emerging role of lncRNAs in cancer	9
1.5 Cyclic nucleotide phosphodiesterases (PDEs)	10
1.6 PDE role in cancer	12
1.7 MPPED2 protein function	13
1.8 The implication of MPPED2 in cancer	14
1.9 Thyroid cancer.....	15
1.10 Breast cancer	16
2. AIMS	19
3. Materials and Methods.....	20
3.1 Human tissue samples.....	20
3.2 Long non-coding RNA Microarray analysis.....	20
3.3 Cell culture and transfection	20
3.4 Plasmids	21
3.5 The Cancer Genome Atlas (TCGA) database	21
3.6 5-Aza-2'-deoxycytidine (5-Aza-dC) treatment.....	21
3.7 Amplicon-Based library preparation and targeted bisulfite sequencing ..	21
3.8 RNA Immunoprecipitation (RIP) assay	22
3.9 Chromatin Immunoprecipitation (ChIP) assay	22
3.10 Immunohistochemical evaluation of a breast tissue microarray (TMA)	23
3.11 RNA extraction and quantitative Real-Time PCR (qRT-PCR)	24
3.12 Western blot	25
3.13 Flow cytometry	25
3.14 Cell migration and invasion assays	25
3.15 Colony formation assay.....	26
3.16 Growth curve assay	26
3.17 Statistical analysis	26

4. Results	27
4.1 Identification of lncRNAs deregulated in PTC	27
4.2 MPPED2 is induced by MPPED2-AS1 and their restoration negatively modulates cell proliferation and migration of thyroid cancer cells	30
4.3 MPPED2-AS1 and MPPED2 are downregulated in human breast cancer samples	33
4.4 MPPED2 promoter is hypermethylated in human breast cancer samples	39
4.5 The lncRNA MPPED2-AS1 positive regulates MPPED2 expression by binding DNMT1	42
4.6 MPPED2 overexpression inhibits breast carcinoma cell growth	44
4.7 Restoration of MPPED2 suppresses the malignant phenotype of BC cells	47
5. Discussion	49
6. Conclusion	53
7. List of publications	54
8. References	56

Abstract

Long non-coding RNAs are a class of heterogeneous non-coding transcripts longer than 200 nucleotides. Recently, it has been shown that they play a pivotal role in several cellular processes exerting regulatory functions at both transcriptional and translational levels. Importantly, the deregulation of lncRNAs has been frequently found in many pathophysiological processes, particularly cancer, considering them as potential molecular biomarkers for cancer.

Here, we analyzed the lncRNAs expression profile of twelve papillary thyroid cancer and four normal thyroid tissues through a lncRNA microarray. By this approach we identified 1560 deregulated lncRNAs with absolute fold change >2 and p -value <0.05 . Additional analysis has been made to improve the quality of the array by setting p -value <0.001 and false discovery rate ≤ 0.01 , and obtaining 12 up- and 44 downregulated lncRNAs. Among them, we focused on the downregulated *MPPED2-AS1* located in antisense position respect to the *MPPED2* gene, which encodes a metallophosphoesterase with tumor suppressor activity. We then investigated in deep their role in cancer.

We found that both these genes are downregulated in malignant thyroid neoplasia. Inhibition of thyroid carcinoma cell growth and migration ability was achieved by the *MPPED2-AS1* and *MPPED2* restoration. Interestingly, *MPPED2-AS1* overexpression can increase *MPPED2* levels. This mechanism was further corroborated in breast cancer. Indeed, we observed that *MPPED2-AS1* and *MPPED2* levels were significantly decreased in breast cancer samples, and this was confirmed by the evaluation of data in The Cancer Genome Atlas. On the other hand, hypermethylation of CpG islands in the *MPPED2* promoter was detected in 87.5% of breast tumors and was significantly associated with a lack of *MPPED2* expression. The treatment with the demethylating agent, 5-Aza-2'-deoxycytidine, partially restored *MPPED2* RNA and protein levels in breast cancer cell lines. Further studies revealed that *MPPED2-AS1* overexpression led to an increased *MPPED2* levels even in breast cancer. Particularly, the lncRNA binds the DNA methyltransferase1 (DNMT1) and, consequently, prevent *MPPED2* promoter in breast cancer cells. Furthermore, the restoration of *MPPED2* expression reduced cell proliferation, migration and invasion capabilities of breast cancer cell lines, suggesting its tumor suppressor role also in breast cancer.

Taken together, these results propose *MPPED2-AS1* and *MPPED2* as novel tumor suppressor in thyroid and breast cancer and reveals that *MPPED2-AS1* positive modulates *MPPED2* expression by reducing its promoter methylation.

1. Background

1.1 Class of non-coding RNAs (ncRNAs)

The central dogma of molecular biology explains the flow of genetic information through which the DNA is transcribed in messenger RNA (mRNA) and subsequently, this latter is translated into protein (Crick 1958). However, the Encyclopaedia of DNA Elements (ENCODE) project has revealed that only 1% of the human genome codes for proteins, leaving the large majority (70-90%) transcribing for RNA with no apparent protein-coding capacity (Ponting *et al.*, 2009). For a long time, these molecules have been considered as “junk RNA”, but nowadays it has become increasingly apparent that they are a central part of gene regulation machinery, and have crucial functionality for normal development, physiology, and disease (Mercer *et al.*, 2009). Thus, the new *era* of non-coding RNA (ncRNA) provides a significant novel perspective on the crucial role of RNA in gene regulation.

Based on the difference in length, ncRNAs can be divided into two main groups: small-ncRNAs (sncRNAs) (fewer than 200 nucleotides), which includes microRNAs (miRNAs), piwi-interacting RNAs (piRNAs), and short-interfering RNAs (siRNAs); and long-non-coding RNAs (lncRNAs) (longer than 200 nucleotides), including natural antisense transcripts, small nucleolar RNAs (snoRNAs), circular RNAs (circRNA) and other types of lncRNAs (Amaral *et al.*, 2008, Collins and Chen 2009, Collins and Penny 2009, Mattick 2009) (Table 1).

The functional relevance of the ncRNAs has been previously well characterized for miRNAs (He and Hannon 2004, Mendell 2005). In fact, in human diseases, it has been proven that epigenetic and genetic mutations in miRNAs and their processing machinery are a hallmark of neurological, cardiovascular, autoimmune, imprinting and monogenic disorders (Croce 2009, Esquela-Kerscher and Slack 2006, Hammond 2007, Nicoloso *et al.*, 2009). However, more recently, even other non-coding protein genes, like piRNAs, snoRNAs, transcribed ultraconserved regions (T-UCRs) and lncRNAs have been demonstrated to have an important contribution to the development of several human diseases (Mercer *et al.*, 2009), highlighting their relevance in many biological processes.

Table 1. Classes of non-coding RNAs (ncRNAs)

<i>Class of non-coding RNAs</i>	<i>Symbol</i>	<i>Length (nt)</i>	<i>Function</i>
Small non-coding RNAs			
sncRNAs			
Small interfering RNAs	siRNAs	20-25	Double-stranded RNA similar to miRNA, operating through RNA interference (RNAi) pathway; promote RNA degradation
Micro-RNAs	miRNAs	21-24	Function in RNA silencing and post-transcriptional regulation of gene expression; may have an extracellular localization
Piwi-interacting RNAs	piRNAs	26-31	Epigenetic and post-transcriptional gene silencing of retrotransposons and other genetic elements in germ-line cells
Long non-coding RNAs			
lncRNAs			
Long intergenic non-coding RNAs	lincRNAs	>200	Involved in epigenetic modification, post-transcriptional processing, modulation of chromatin structure
Transcribed ultraconserved region	T-UCR	≈50-570	Frequently located at fragile sites and cancer-associated genomic region; possibly regulated by miRNA
Circular RNAs	circRNAs	≈100-1600	Covalently closed RNA ring, some have coding functions, potential gene regulation and miRNA “traps”
Small nucleolar RNAs	snoRNAs	60-300	Guide chemical modifications of other RNAs (rRNA, tRNA, snRNA)

1.2 Characteristics of lncRNAs

The findings that many genomic sequences in superior organisms are transcribed in a developmental- and tissue-regulated manner (Carninci *et al.*, 2005, Kapranov *et al.*, 2007), has fuelled a race to characterize all the different types of non-protein coding genes transcribed in human cells. However, even though most of the studies have focused on the class of sncRNAs, the lncRNAs are also gaining importance in human biology. LncRNAs are considered as a heterogenic class of ncRNA molecules longer than 200 nucleotides (Wang *et al.*, 2011). Like messenger RNAs (mRNAs), lncRNAs usually are transcribed by RNA polymerase II (Pol II) (although often transcribed by RNA polymerase III), being 5'-capped, polyadenylate and alternatively spliced (Guttman *et al.*, 2009). However, in comparison with the protein-coding genes, they are expressed at relatively low levels, exhibit poor evolutionary conservation and show cell- and tissues-type specific expression (Cabali *et al.*, 2011, Derrien *et al.*, 2012). As well, lncRNAs are found in many different places within the cells, including chromatin, nucleus, nucleolus, cytoplasm, and mitochondria (Cabali *et al.*, 2015, Rackham *et al.*, 2011). The subcellular localization is an important feature that provides information regarding the functional roles of lncRNAs. Furthermore, based on the different genomic position and the position relative to the neighbouring protein-coding

genes, lncRNAs can be classified into five categories (Ponting *et al.*, 2009, Rinn and Chang 2012, Yan and Wang 2012) (Figure 1):

- (i) intergenic lncRNAs (lincRNAs) are positioned between two protein-coding genes,
- (ii) bidirectional lncRNAs are located from the bidirectional transcription of protein-coding genes,
- (iii) intronic lncRNAs are ncRNAs molecules that overlaps into an intronic region of a protein-coding gene in either sense or antisense orientation,
- (iv) antisense lncRNAs (or natural antisense transcripts, NATs) are lncRNAs transcribed in the opposite direction of protein-coding genes and overlap at least one coding exon,
- (v) sense lncRNAs are transcripts that overlap with the sense strand of protein-coding genes.

Additionally, recent studies indicate that either lncRNA classification or localization can provide information about the potential mechanisms of action of lncRNAs (Khalil *et al.*, 2009, Long *et al.*, 2017), even though it is not clear yet how they can reflect their biological function.

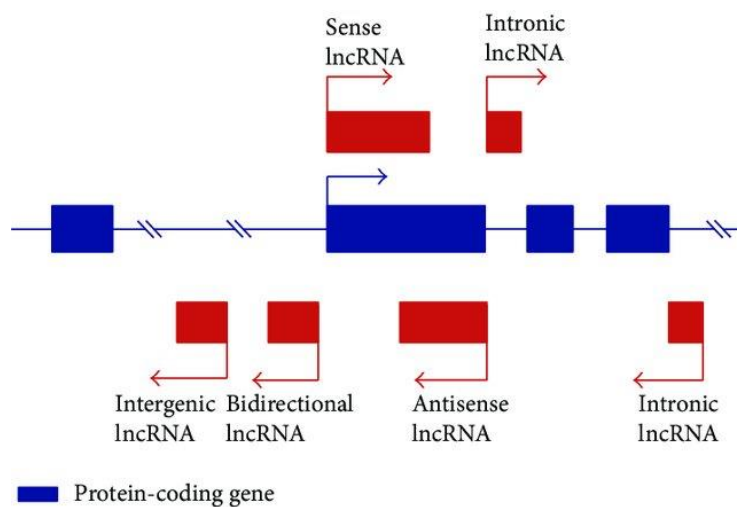


Figure 1. lncRNAs classification based on their genomic orientation. lncRNAs are subdivided into five categories based on to their genomic localization with respect to neighbouring protein-coding genes. Intergenic lncRNAs (lincRNAs) are lncRNAs transcribed intergenically from protein-coding genes. One definition required lincRNAs to be at least 1 kb away from protein-coding genes. Bidirectional lncRNAs are transcripts that originate from the opposite strand of the same promoter of a protein-coding gene. Intronic lncRNAs are RNA molecules that originate inside of an intron of a protein-coding gene in either direction (sense or antisense orientation) and terminate without overlapping exons. Antisense lncRNAs are lncRNAs transcripts from the antisense strand of the annotated protein-coding gene and can overlap either with exon or intron regions. Sense lncRNAs originates in the same strand of protein-coding genes and overlapping with other gene located on the same strand. lncRNAs are shown in red box. From: Losko *et al.*, 2016, Long Noncoding RNAs in Metabolic Syndrome Related Disorders, *Mediators of Inflammation*, 2016 Nov 2;2016(5365209).

1.3 Molecular mechanisms of lncRNAs action

Over the last decade, lncRNAs have caught the attention of molecular biologists for their implication in important biological processes, including differentiation (Guttman *et al.*, 2011), epigenetic modification (Ciado *et al.*, 2006, Tsai *et al.*, 2010), and tumorigenesis (Gupta *et al.*, 2010). Importantly, lncRNAs have been defined as fine-tuner of gene regulation networks since they exert regulatory function at early ever event of gene expression program, acting at both transcriptional and post-transcriptional levels through a variety of diverse mechanisms (Batista and Chang 2013, Fatica and Bozzoni 2014) (Figure 2). Indeed, they can regulate the expression of neighbouring (*cis*-regulation) and/or distant (*trans*-regulation) genes *via* chromatin remodeling and histone modifications (Rinn and Chang 2012). Also, lncRNAs can act as decoys by interacting with transcription factor and preventing their binding on the regulatory DNA elements or keeping proteins away from chromatin by inducing histone modifications or DNA methylation (Mercer and Mattick 2013). They may serve even as scaffolds, and show heterogenic regulatory functions interacting with DNA, RNA or proteins. Further, lncRNAs act by modulating mRNAs translation (Yoon *et al.*, 2012), splicing (Tripathi *et al.*, 2010), mRNA degradation (Gong and Maquat 2011), and protein stability. Besides, lncRNA could serve as a competitive endogenous RNA (ceRNA) preventing the binding of miRNA to their specific target mRNA. Since more cases of regulation by lncRNAs are still far from being uncovered, it is possible to speculate that the lncRNA class will finally compete with the snRNA class and proteins as main regulators of genetic information.

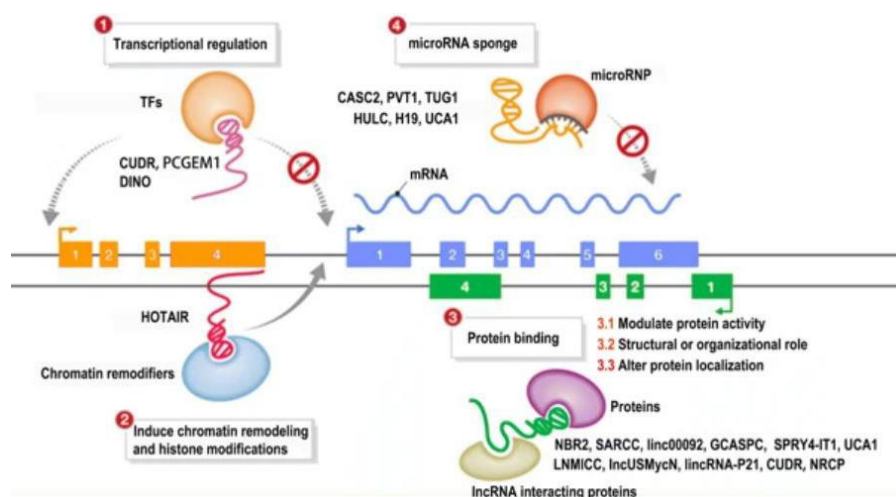


Figure 2. Different mechanisms of lncRNA function. Various studies have elucidated several mechanisms of action by lncRNAs. For each molecular mechanism of function, an example is reported in the brackets. 1) lncRNAs act as decoys-decoy through the interaction with transcription factors and preventing its action on the target DNA. 2) lncRNAs regulate gene expression by

recruiting chromatin modifiers. 3) LncRNAs modulate different biological processes by binding of the RNP component, regulating the activity and/or localization of the protein and playing a role in the organization within the nucleus. 4) LncRNAs serve as ceRNA for miRNA acting as sponges by taking the miRNAs away from their mRNA targets. 5) LncRNAs regulate the translation and/or degradation of their mRNA targets. 6) LncRNAs can regulate the splicing of pre-mRNA. lncRNA, long non-coding RNA; mRNA, messenger RNA; RNP, Ribonucleoprotein; ceRNA, competitor endogenous RNA. From: Sun *et al.*, 2018, Emerging roles of long non-coding RNAs in tumor metabolism. *Journal of Hematology & Oncology*, 2018 Apr 20;17(1).

1.4 Emerging role of lncRNAs in cancer

Cancer development and progression are a genetic disease that can be mediated through many mechanisms involving lncRNAs (Cheetham *et al.*, 2013, Gibb *et al.*, 2011, Hauptman and Glavac 2013, Mitra *et al.*, 2012, Zhang *et al.*, 2013). The key role played in malignant transformation by these ncRNAs has been widely studied, and it involves a variety of processes as epigenetic modification, either activation of oncogenic or inactivation of tumor-suppressive pathways, and crosstalk with other RNA subtypes (Calin *et al.*, 2007, Gao *et al.*, 2016, St Laurent *et al.*, 2015). A great number of lncRNAs have been functionally associated with human cancers (Gutschner and Diederichs 2012), and frequently, alteration of lncRNAs exerts impacts on cellular behaviour commonly deregulated in cancer as cell proliferation, resistance to apoptosis, induction of angiogenesis, promotion of metastasis, and evasion of tumor suppressors (Brunner *et al.*, 2012, Gutschner and Diederichs 2012). Some modes of action in cancer of lncRNAs are summarized in Table 2. Although lncRNAs are hardly functionally explained (Quek *et al.*, 2015), their mechanisms of action can be distinguished based on their impact on chromatin structure and methylation modification, the stability of proteins and complexes or by serving as a sponge for miRNA inhibition (Quinn and Chang 2016). In fact, as discussed earlier, lncRNAs can modify the expression of target genes by interacting with chromatin remodelling complexes (Fatica and Bozzoni 2014). One example of lncRNA that acts through chromatin modification is the antisense lncRNA *ANRIL* localized in the *INK4* locus. In fact, *ANRIL* acts as scaffold inducing transcriptional repression of *INK4b-ARF-INK4a* locus by recruiting and interacting with PRC1 and PRC2, two proteins of the Polycomb Repressive complex that play key role in transcriptional silencing of genes (Aguilo *et al.*, 2011, Kotake *et al.*, 2011). Lately, studies have demonstrated that lncRNAs are involved in epigenetic modification, including DNA methylation (Lee 2012, Schaukowitch and Kim 2014), one of the most common epigenetic changes associated with various diseases, particularly with cancer (Davis and Uthus 2004, Jones 1996, Laird and Jaenisch 1994, Liu *et al.*, 2003). Another outstanding example comes from the *large intergenic long non-coding RNA p21 (lincRNA-p21)* that impairs somatic cell reprogramming by maintaining H3K9me3 and/or CpG methylation at pluripotency genes promoter (Bao *et al.*, 2015).

Moreover, a significant number of lncRNAs exerts their oncogenic or tumor suppressor activity through direct interaction with proteins or protein complexes as scaffolds or allosteric activators/inhibitors (Ling *et al.*, 2013, Takayama *et al.*, 2013, Wang *et al.*, 2013). Notably, it has been extensively documented that deregulation of lncRNAs is strictly associated with clinicopathological outcome and prognosis, making them a potential diagnostic and prognostic markers in the pathology of cancer disease (Flynn and Chang 2014, Hu *et al.*, 2012, Rossi and Antonangeli 2014). Overall, enhanced knowledge of lncRNAs in cancer will shed the light of understanding in cancer biology, and lncRNA-based therapies could become an important healthcare strategy for the treatment of various types of cancers.

Table 2. Mode of action of long non-coding RNAs (lncRNAs) in human cancer

<i>Cancer Hallmark</i>	<i>lncRNA</i>	<i>Mode of Action</i>
I) Sustaining proliferative signaling	<i>SRA</i> <i>PCAT-1</i> <i>RN7SK</i> <i>ncRNAs derived from cell cycle gene promoters</i> <i>KRASPI</i> <i>HMGAIPIs</i> <i>PR Antisense</i> <i>BRAFPI</i>	Transcriptional co-activator Regulating gene expression Regulating transcription Unknown miRNA sponge miRNA sponge Regulating gene expression miRNA sponge
II) Evading growth suppressors	<i>PSF-interacting RNA</i> <i>ANRIL</i> <i>GASS</i> <i>lincRNA-p21</i> <i>E2F4 antisense</i>	Modulating protein activity Chromatin remodelling Competitor Transcriptional co-repressor Regulating gene expression
III) Enabling replicative immortality	<i>TERC</i> <i>TERRA</i>	RNA primer Enzymatic inhibitor
IV) Activating invasion and metastasis	<i>MALAT1</i> <i>HOTAIR</i> <i>HULC</i> <i>BC2000</i>	Modulating protein activity, sensor, scaffold Chromatin remodelling miRNA sponge Translation modulator
V) Inducing angiogenesis	<i>aHIF</i> <i>sONE/NOS3AS</i> <i>tie-1AS</i> <i>ncR-uPAR</i>	RNA decay RNA decay RNA decay Regulating gene expression
VI) Resisting cell death	<i>PCGEMI</i> <i>CUDR</i> <i>Uc.73A(P)</i> <i>SPRY4-IT1</i> <i>PANDA</i> <i>LUST</i> <i>PINC</i>	Regulating gene expression Regulating gene expression Unknown Unknown Modulating protein activity RNA-Splicing Unknown

1.5 Cyclic nucleotide phosphodiesterases (PDEs)

The phosphodiesterases (PDEs) are a group of enzymes able to breakdown the phosphodiester bond. Usually, PDEs refer to cyclic nucleotide phosphodiesterases, proteins with key role in intracellular signaling through the hydrolysis of cyclic adenosine monophosphate (cAMP) and/or cyclic guanine monophosphate (cGMP) (Sutherland and Rall 1958), second messengers molecules

implicated in the control of important cellular functions, such as cell proliferation, cell growth, apoptosis and differentiation (Piazza *et al.*, 2001). The cyclic nucleotide PDEs, in turn, are divided into three classes based on different aminoacidic sequences and differences in their catalytic domain (Figure 3).

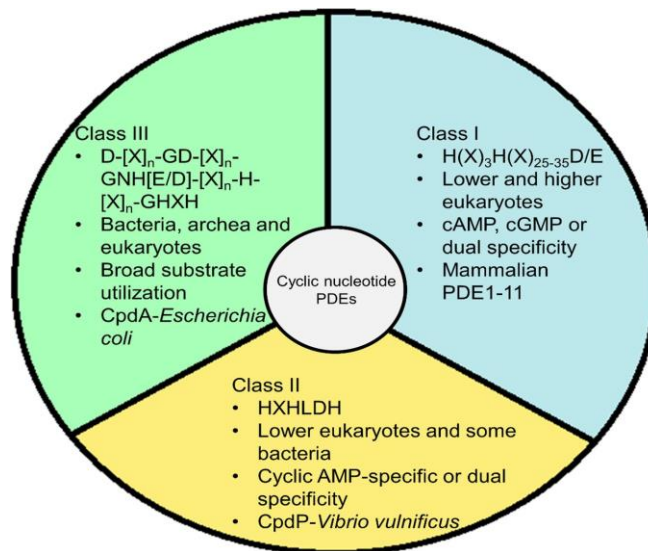


Figure 3. Classification of cyclic nucleotide PDEs. The cyclic nucleotide PDEs are subdivided into three classes based on their sequences. The presented graph shows for each class the conserved sequence motif, the phyletic distribution and the substrate (cAMP or cGMP) specificity. An example for the three classes it has been reported. From: Matange, 2015, Revisiting bacterial cyclic nucleotide phosphodiesterases: cyclic AMP hydrolysis and beyond, *FEMS Microbiology Letters*, 2015 Sept 15; 362(22).

The class I PDE is the most extensively studied family, harboring the H(X)₃H(X)₂₅₋₃₅D/E motif (Richter 2002). These enzymes have been found either in lower and higher eukaryotes and their exclusive function is the regulation of cAMP and cGMP levels. In fact, they can hydrolyze both cAMP and cGMP or be specific for cAMP and cGMP (Francis *et al.*, 2011, Francis *et al.*, 2001, Mehats *et al.*, 2002).

The class II PDE, instead, is characterized by the HXHLDH signature (Richter 2002). They have been identified in lower eukaryotes, including protozoa and yeasts, and some bacteria like *Vibrio* (Callahan *et al.*, 1995, Kimura *et al.*, 2011, Powell *et al.*, 2014). Similar to class I, the enzymatic activity could be specific or not for the second messengers (Callahan *et al.*, 1995, Kimura *et al.*, 2011).

Finally, the class III PDE represents a ubiquitous family of enzymes, even though initially it has been thought to be restricted only to bacteria (Powell *et al.*, 2014, Richter 2002). More in deep, this class belongs to metallophosphoesterase (MPE) superfamily since they share the same motif characterized by five blocks of conserved residues (D-[X]_n-GD-[X]_n-GNH[E/D]-[X]_n-H-[X]_n-GHXH) (Richter 2002) (Figure 4).

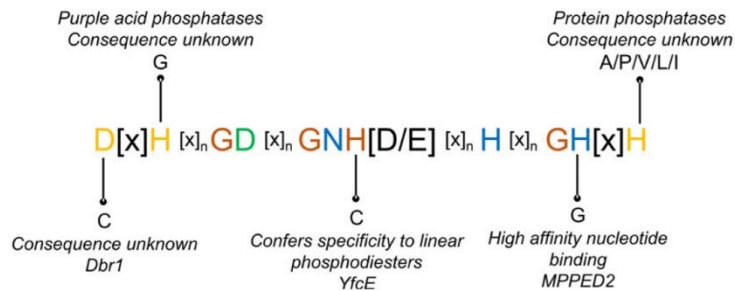


Figure 4. Conserved sequence motif in MPEs. Schematic representation of the MPE motif showing conserved residues and some variations seen in these residues. In the graph are reported all five blocks of conserved residues. It is possible to note that aminoacidic changes could prompt the loss of the PDE class III enzymatic activity. Matange *et al.*, 2015, Metallophosphoesterases: structural fidelity with functional promiscuity. *Biochemical Journal*. 2015 Apr 2;467 (2).

The catalytic function of class III PDE is dependent on the binding of two metal ions in the active site (Fuchs *et al.*, 2010, Imamura *et al.*, 1996, Kimura *et al.*, 2009, Mathieu-Demaziere *et al.*, 2013, Podobnik *et al.*, 2009, Shenoy *et al.*, 2007), and importantly, residues changes in the catalytic domain could cause the complete loss of the hydrolytic activity (Matange *et al.*, 2015). Furthermore, despite their high degree of homology, MPE proteins show several different functions (Matange 2015). In fact, they can act as nucleases, phosphoprotein phosphatases, cyclic nucleotide PDE or serve as a scaffold for protein-protein interaction, and, thereby, all the components of this group have key roles in many different activities such as DNA repair, cyclic nucleotide metabolism and RNA processing (Connelly and Leach 2002, Ren *et al.*, 2009).

1.6 PDE role in cancer

In the last decade, a significant number of studies have elucidated the influence of PDEs in cancer development and progression (Levy *et al.*, 2011, Maurice *et al.*, 2014). In fact, increased PDE expression has been found in many tumors such as colon cancer (Hirsh *et al.*, 2004), breast cancer (Zhang *et al.*, 2019), and lung cancer (Whitehead *et al.*, 2003). For example, PDE7B has been found upregulated in chronic lymphocytic leukemia (CLL) where it is required for CLL cell survival (Zhang *et al.*, 2011, Zhang *et al.*, 2008). Also, PDE10 has been found overexpressed in colon cancer where it increased cell proliferation and activated T-cell factor (TCF) transcriptional activity (Li *et al.*, 2015). Specifically, elevated PDE levels lead to an impairment of cAMP and cGMP within the cells (Hirsh *et al.*, 2004), thus inducing an aberrant cyclic nucleotide signaling that plays a pivotal role in tumorigenesis (Ahn *et al.*, 2005). Indeed, several findings revealed that cAMP may suppress cell proliferation by blocking extracellular signal-regulated kinase (ERK) signaling (Tortora and Ciardiello 2002), or by inhibiting various oncogenes like Myc and erbB-2 (Wang *et al.*, 2005). Furthermore, low cAMP levels have been found in tumoral cells, thus underlining a key contribution of PDE

deregulation in cancer progression (Cho-Chung and Nesterova 2005, Drees *et al.*, 1993). Given this scenario, PDE inhibitors are useful drugs for the treatment of various types of cancer (Savai *et al.*, 2010) acting by inhibiting tumoral growth, inducing apoptosis (Page and Spina 2011), modulating T-cell responses (Bjorgo *et al.*, 2011) and monocyte differentiation (Hertz and Beavo 2011). Thereby, PDE inhibitors increased chemotherapeutic efficacy and can be used as monotherapy or in combination with other chemotherapeutic agents to have beneficial effects and overcome drug resistance in cancer (Das *et al.*, 2010).

1.7 *MPPED2* protein function

Metallophosphodiesterase-domain-containing protein 2 (MPPED2) is a member of MPE superfamily, representing the first evidence of Class III PDE in mammals with a highly evolutionary degree of sequence conservation throughout the evolution (Tyagi *et al.*, 2009). The *MPPED2* gene is located on human chromosome 11p13 in a region that comprises several developmental genes, likewise *WT1*, *BDFN-1*, *FSHB* and *PAX6* genes (Schwartz *et al.*, 1995) (Figure 5).

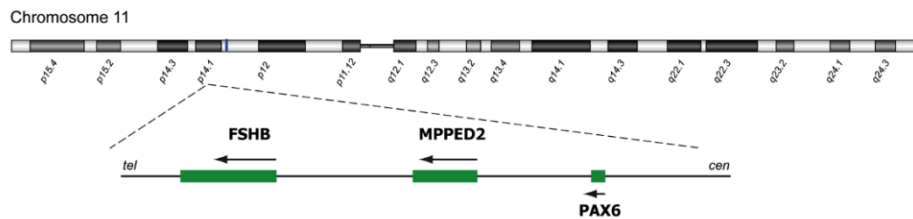


Figure 5. Genetic locus of MPPED2. The present graph shows the localization of *MPPED2* gene on human chromosome 11p13. In particular, *MPPED2* gene is located between *FSHB* and *PAX6* genes, in a region whose deletion is associated with WAGR syndrome.

In particular, the deletion of this locus has been found responsible for the development of WAGR syndrome, a rare genetic disorder in which patients are predisposed to develop Wilms tumor, aniridia, genitourinary anomalies, and mental retardation (Schwartz *et al.*, 1995). More in detail, its expression is predominant in the fetal brain, suggesting its contribution to the nervous system development (Schwartz *et al.*, 1994). However, extensive biochemically and structurally studies showed that MPPED2 has poor hydrolytic activity against cAMP and cGMP *in vitro* due to an aminoacidic substitution in the MPE active site, where a glycine (Gly) residue at the position 252 (G252) substitutes the highly conserved histidine (His) (Matange *et al.*, 2015) (Figure 6). Indeed, it is known that the preservation of His residue is fundamental for the binding of metal ions in the active site, and therefore, for the enzymatic activity. Thus, as a consequence of the unique G252 substitution, the MPPED2 active site naturally binds AMP or GMP with a strong affinity, almost abrogating MPPED2 hydrolytic function (Dermol *et al.*, 2011). These observations support the idea that MPPED2 role may not be restricted only to hydrolyze phosphodiester substrates but, as already demonstrated for other MPE

family members, whose catalytic activity is completely lost (Swarbrick *et al.*, 2011), MPPED2 may act as a scaffold protein.

Enzyme	Active-site residues							
MPPED2	Asp ⁶⁵	His ⁶⁷	Asp ⁸⁶	Asn ¹¹⁷	His ¹¹⁸	His ²¹³	Gly ²⁵²	His ²⁵⁴
Rv0805	Asp ²¹	His ²³	Asp ⁶³	Asn ⁹⁷	His ⁹⁸	His ¹⁶⁹	His ²⁰⁷	His ²⁰⁹
Mre11	Asp ⁸	His ¹⁰	Asp ⁴⁹	Asn ⁸⁴	His ⁸⁵	His ¹⁷³	His ²⁰⁶	His ²⁰⁸
GpdQ	Asp ⁸	His ¹⁰	Asp ⁵⁰	Asn ⁸⁰	His ⁸¹	His ¹⁵⁶	His ¹⁹⁵	His ¹⁹⁷
Lmo2642	Asp ⁴⁷	His ⁴⁹	Asp ¹⁰¹	Asn ¹³⁴	His ¹³⁵	His ²⁴³	His ²⁸¹	His ²⁸³

Figure 6. Active site aminoacidic residues in MPEs. Summary of the active site residues found in some characterized MPEs highlighting deviation from the MPE motif consensus of MPPED2 aminoacidic sequence. In particular, in red it is reported the unique replacement of MPPED2 where a glycine (Gly) residue substitutes the highly conserved histidine (His). From: Matange *et al.*, 2015, Metallophosphoesterases: structural fidelity with functional promiscuity. *Biochemical Journal*. 2015 Apr 2;467 (2).

1.8 The implication of MPPED2 in cancer

MPPED2 gene also showed opposite behaviour respect to the other PDE members. Indeed, although some class I PDEs have been found mainly upregulated in cancer, showing oncogenic activity, several studies have reported that MPPED2 exhibits anti-oncogenic role in several human cancer as neuroblastoma (Liguori *et al.*, 2012), cervical cancer (Zhang *et al.*, 2016) and oral squamous carcinomas (Shen *et al.*, 2016). In fact, *in vivo* and *in vitro* studies showed that MPPED2 reduces cell proliferation, induces cellular retardation in the G1/S phase and induces apoptosis, and its expression is negatively regulated by mir-448 in oral squamous cell carcinoma, thus underlining that the loss of MPPED2 expression might contribute to the process of human carcinogenesis. Remarkably, recent data indicated that decreased *MPPED2* expression in cancer could be due to epigenetic modification. In fact, Liguori and colleagues found an increased *MPPED2* expression after the treatment with a demethylating agent (Liguori *et al.*, 2012). This observation was further corroborated in colon cancer, in which was observed a strict correlation with hypermethylation in *MPPED2* promoter and colorectal neoplastic progression (Gu *et al.*, 2019), underlining that epigenetic mechanism could be one of the main mechanisms that lead to an *MPPED2* reduction in cancer. All these findings further corroborating the tumor suppressor contribution of *MPPED2* gene in cancer development, considering MPPED2 as a new enzyme with unique opposite functions in comparison with the other PDE family members (Figure 7).

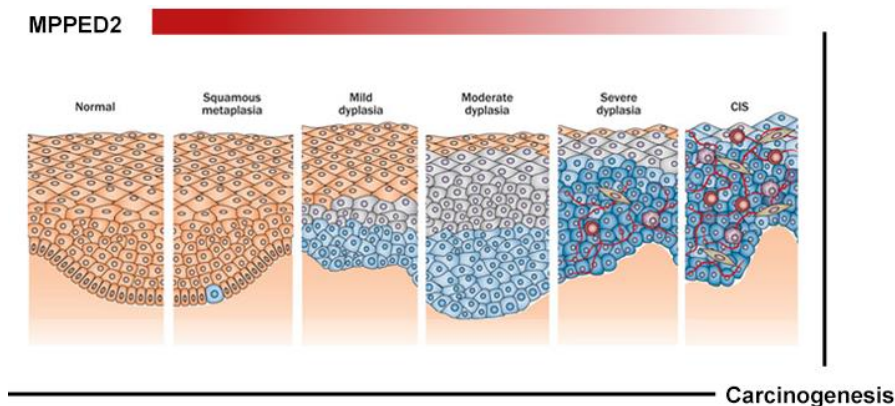


Figure 7. MPPED2 in cancer. Several recent studies reported that the MPPED2 expression levels decrease during the tumorigenesis process, thus suggesting a tumor suppressor role for MPPED2 protein.

1.9 Thyroid cancer

Thyroid cancer (TC) represents the most common malignancy derived from the endocrine system, accounting for 1% of all human carcinomas with a significant overall incidence in the last decades (Fagin and Wells 2016). Usually, TC represents the sixth most common type of cancer in women, with a male to female incidence ratio of 1:3. The age of diagnosis is around 40/50 years of age for the women, whereas the diagnosis in men is around their 60s or 70s. About 2% of TC occurs in children and teens. TCs that originate from thyroid follicular cells are responsible for about 95% of all cases and consist of several histological subtypes with a wide range of lesions subdivided into the well-differentiated papillary (PTC) and follicular thyroid carcinomas (FTC), poorly differentiated thyroid cancer (PDTCs) and undifferentiated anaplastic thyroid carcinomas (ATC) (Nikiforov 2011). Among them, PTCs account for more than 85% of all total cases, while FTCs represent 10% of TCs. The PDTCs, that are more aggressive than PTCs and FTCs, account for only 1-15% of total cases, whereas, despite the ATC subtypes are the less common thyroid neoplasia (<1%), they represent the most aggressive and lethal thyroid neoplasia in mankind.

TC histotypes of different grade of malignancy are considerably linked with the different genetic alterations on some genes and pathways. Particularly, thyroid carcinogenesis and TC progression are associated to somatic point mutations on genes that once mutated trigger the hyperactivation of mitogen-activated protein kinase (MAPK) and phosphoinositide 3-kinase (PI3K) signaling pathways (Figure 8). The genetic alterations regarding predominantly *BRAF* (*B-rapidly accelerated fibrosarcoma*), *RAS*, *RET*, and *NTRK1/3* genes (Saji and Ringel 2010, Xing 2010). Intriguingly, the most clinically relevant hallmark includes point mutations in *BRAF* and *RAS* and *RET/PTC* and *PAX8/PPAR γ* rearrangements. Particularly, the most common genetic alterations in the well-differentiated TC regarding mutations in *BRAF* and *RAS*, together

with *RET/PTC* rearrangement. Specifically, PTC is known to harbour *BRAF* most commonly, followed by *RAS* and *RET/PTC* fusion, whereas FTC is characterized by the presence of either *RAS* or *PAX8/PPAR γ* (Dwight *et al.*, 2003, Nikiforova *et al.*, 2003, Nikiforova and Nikiforov 2009, Vasko *et al.*, 2003, Xing 2007). In fact, in PTC patients (60%), the *BRAF*^{V600E} mutation is the most frequent alteration. The somatic mutations in *BRAF* gene have been found only in PTC and some PTC-derived ATCs, and it is absent in FTC or benign thyroid nodules. (Kunstman *et al.*, 2015, Xing *et al.*, 2009). Also, in PTC aetiology the *RET/PTC* rearrangements seem to be an early event in thyroid carcinogenesis, with about 10–20% of *RET* fusions detected in PTC patients (Kunstman *et al.*, 2015, Xing *et al.*, 2009). Furthermore, the *RAS* genes (*H-RAS*, *N-RAS*, *K-RAS*) present somatic point mutations in all TC histotypes: FTC (40–53%), PTC (0–20%), PDC and ATC (20–60%) (Di Cristofaro *et al.*, 2006, Esapa *et al.*, 1999, Kondo *et al.*, 2006, Kunstman *et al.*, 2015, Santarpia *et al.*, 2010, Vasko *et al.*, 2003). As well, *RAS* mutations together with *TERT* promoter mutations (C228T and C250T) have been linked with more malignant and recurrent thyroid neoplasia and patient mortality, particularly in PTC patients.

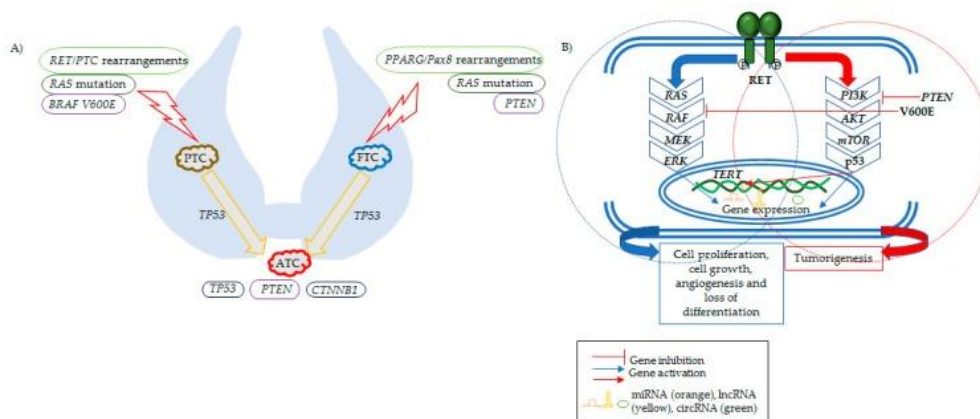


Figure 8. Genetic alterations involved in TC histotypes. (A) In the figure is shown the causative genetic events of TC histotypes. PTCs harbour *BRAF*^{V600E}, *RAS* mutations, and/or *RET/PTC* fusions. FTCs present *RAS* mutations, *PPAR γ /Pax8* rearrangements, and *PTEN* inactivating genetic alterations or deletions. ATCs are characterized by *TP53* inactivation and *PTEN*, *CTNNB1* mutations. (B) The figure shows the key molecular signaling pathways deregulated in TC. On the left: MAPK pathway, which is activated in most TC after genetical alterations. During thyroid carcinogenesis, events of cell proliferation, cell growth, angiogenesis, and differentiation are deregulated. On the right: thyroid tumor progression is due to molecular signaling pathways altered, including the *PI3K/mTOR* pathway, *TP53* tumor suppressor, and mutations in *TERT* promoter. From: Luzón-Toro *et al.*, 2019, Influencers on Thyroid Cancer Onset: Molecular Genetic Basis, *Genes*, 2019 Nov 8;10(11).

1.10 Breast cancer

Breast cancer (BC) is the most common female tumor worldwide representing the second leading cause of mortality in women due to cancer. It

comprises a wide spectrum of lesions, going from benign neoplasia, as fibroadenoma, to more aggressive forms. From a histological point of view, these latter can originate from lobular or ductal cells, so allowing the formation of lobular or ductal carcinomas, respectively, both further classified in invasive and non-invasive tumors (Ellis *et al.*, 2013). However, it has been widely demonstrated that several molecules and pathways are involved and deregulated in the development of sporadic and hereditary breast cancers like growth factors and their receptors, proteins involved in the control of cellular proliferation and the DNA damage repair, and molecules leading to the activation of specific signal transduction mechanisms (Vogelstein and Kinzler 1994). Most of these proteins are nowadays considered as genetic markers. In particular, the BRCA1/2 mutational status, and the expression of estrogen receptor (ER), progesterone receptor (PR), and human epidermal growth factor receptor 2 (HER2) are used in clinical oncology to make the correct diagnosis and to establish the right treatment for the specific disease (Deroo and Korach 2006, Gao and Nawaz 2002, Hynes and Stern 1994, Miecznikowski *et al.*, 2010). Furthermore, BC is mainly characterized by the presence and/or absence of ER, PR, and HER2 (Blows *et al.*, 2010, Vallejos *et al.*, 2010). These parameters determine the aggressiveness of the tumor, and their combination defines the main molecular BC subtypes that in turn are divided into luminal A (Lum A; ER+ and/or PR+, HER2-, with low levels of the protein Ki-67), luminal B (Lum B; ER+ and/or PR+, HER2+, with high levels of Ki-67), human estrogen receptor growth factor 2 (HER2; ER-, PR-, HER2+), and triple-negative breast cancer (TNBC; ER-, PR-, HER2-) (Table 3). In particular, both Lum A and Lum B cancers depend on estrogen for the growth, and the patients usually efficiently respond to endocrine therapy. The HER2 subtype, instead, typically showed worse prognosis than the luminal ones, even if they are often successfully treated with targeted therapies aimed at the HER2 protein, such as Herceptin. Finally, TNBC subtypes are common in women with BRCA1 gene mutations. TNBC is considered the most aggressive subtype with the worst prognosis, mainly owing to the fewer useful targeted strategies to treat TNBC (Kondov *et al.*, 2018).

Table 3. Molecular classification of breast cancer (BC) subtypes.

<i>BC subtype</i>	<i>Hormonal status</i>		<i>HER2</i>	<i>PI (Ki-67)</i>
	<i>ER</i>	<i>PR</i>		
Luminal A	+	or +	-	<14%
Luminal B	+	or +	+	≥14%
HER2	-	-	+	Any
TNBC	-	-	-	Any

ER: estrogen receptor; PR: progesterone receptor; HER2: Human epidermal growth factor receptor 2,

PI: Proliferation index, +: Positive; -: Negative.

Nevertheless, these markers are still insufficient to predict the tumor prognosis suggesting that patients could be over- or under-treated (Cianfrocca and Gradishar 2009). In fact, although surgery and chemotherapy are nowadays the most effective tools for BC treatment, tumor relapse might occur within 5 years and recurrent disease is frequently more resistant to chemotherapy due to specific genetic alterations that lead to the deregulation of biological processes resulting in the acquisition of drug resistance. For this reason, the new challenge of cancer research in the last years is represented by the identification of new molecular markers whose expression could be correlated with tumor stages, response to anti-neoplastic treatments and drug-resistance.

2. AIMS

Accumulating evidences have demonstrated that lncRNAs are key regulators of gene expression and cell biology. Additionally, it is well known that the lncRNAs are closely linked to the occurrence and development of various types of cancers, showing potential roles in both oncogenic and tumor-suppressive pathways. In fact, through advancements in cancer-transcriptome profiling, it has become clear that the deregulation of lncRNAs impacts different cellular processes, as proliferation, dedifferentiation, migration, and invasion.

Given this scenario, the present study aims to investigate the role of the lncRNAs in cancer. In particular, this study has been focused on the functional characterization of two novel genes: the antisense lncRNA *MPPED2-AS1* and its associate *MPPED2* gene. To identify new players in carcinogenesis, we evaluated whether *MPPED2-AS1* and *MPPED2* downregulation is a general event in cancer analyzing their expression in TC and BC. Additionally, this study proposes even to explore in detail the mechanism by which *MPPED2-AS1* regulates the *MPPED2* gene and the consequences of this new mechanism especially in the process of carcinogenesis.

This dissertation is based upon the following publications:

Sepe R, **Pellecchia S**, Serra P, D'Angelo D, Federico A, Raia M, Cortez Cardoso Penha R, Decaussin-Petrucci M, Del Vecchio L, Fusco A, Pallante P. The Long Non-Coding RNA RP5-1024C24.1 and Its Associated-Gene MPPED2 Are Down-Regulated in Human Thyroid Neoplasias and Act as Tumour Suppressors. *Cancers (Basel)*. 2018 May 18

Pellecchia S, Sepe R, Federico A, Cuomo M, Credendino SC, Pisapia P, Bellevicine C, Nicolau-Neto P, Severo Ramundo M, Crescenzi E, De Vita G, Terracciano LM, Chiariotti L, Fusco A, Pallante P. The Metallophosphoesterase-Domain-Containing Protein 2 (MPPED2) Gene Acts as Tumor Suppressor in Breast Cancer. *Cancers (Basel)*. 2019 Jun 8

3. Materials and Methods

3.1 Human tissue samples

The whole set of human thyroid carcinoma specimens used was provided by the Service d'Anatomie et Cytologie Pathologiques, Centre de Biologie Sud, Groupement Hospitalier Lyon Sud, Pierre Bénite, France. The activity of biological samples conservation was declared under the number DC-2011-1437 to the Ministry of Research, to the committee of people's protection of south-east IV and to the Health Regional Agency. The activity of biological material cession was agreed upon by the Ministry of Health under the number AC-2013-1867.

Normal and neoplastic human breast tissues were obtained from surgical specimens and immediately frozen in liquid nitrogen. Breast samples were kept frozen until required for nucleic acid extraction. Breast tissue samples were collected at the Institute of Pathology, University of Basel, Switzerland. The study was conducted under the approval of the local ethical committee (#78-09). Informed consent was obtained from all patients.

3.2 Long non-coding RNA Microarray analysis

Total RNA extracted from 12 PTC samples and 4 normal thyroid tissues was hybridized to the Human LncRNA Microarray Version 3.0 of the Arraystar company (Rockville, MD, USA). This system is based on probes able to recognize specific exons or splice junction of each lncRNA. The expression analysis was performed by comparing the average of the expression levels observed in 12 PTC samples with the average of the expression levels observed in four normal thyroid tissues. Bioinformatic analyses were performed by the Arraystar company based on the following databases: Refseq, UCSC, GENCODE, RNAdb, NRED, UCR, lincRNA catalogs.

3.3 Cell culture and transfection

Human cancer cell lines MDA-MB-231, SKBR3, TPC-1 and FRO were cultured in Dulbecco's Modified Eagle Medium (DMEM) (Sigma-Aldrich, St. Louis, MO, USA) supplemented with 10% foetal bovine serum (FBS) (Euroclone, Milan, Italy), 1% L-glutamine, 1% penicillin/streptomycin (Sigma-Aldrich). Cells were kept at 37 °C under 5% CO₂ atmosphere. Lipofectamine 2000 (Life Technologies, Grand Island, NY, USA) reagent was used to transfect MDA-MB-231, SKBR3 and FRO cells according to the manufacturer's instructions, whereas TPC-1 cells were transfected using Fugene HD reagent (Promega, Fitchburg, WI, USA). For stably-expressing cell lines, G418 (Life Technologies) was used to stably restored *MPPED2-AS1* expression, whereas hygromycin (Sigma-Aldrich), was used to stably restored *MPPED2* levels.

3.4 Plasmids

The expression vector encoding human *MPPED2* gene was generated by cloning cDNA sequence in the pcDNA3.1/Hygro (+) vector (Life Technologies) using HindIII and NotI restriction sites. After cloning, the plasmid was subjected to sequencing (Eurofins Genomics, Vimodrone, Italy) and *MPPED2* expression was validated by qRT-PCR and Western blot analyses. The expression vector encoding human *MPPED2-AS1* was obtained by cloning the lncRNA sequence in the pCMV6-AC-GFP vector (Origene Technologies, Rockville, MD, USA) using the HindIII and XhoI restriction sites.

3.5 The Cancer Genome Atlas (TCGA) database

The expression data for PTC and BC samples used in this study, were obtained from The Cancer Genome Atlas (TCGA) by using web-based software Wanderer (Diez-Villanueva *et al.*, 2015). The whole cohort of PTC samples used for *MPPED2* includes a total of 498 thyroid tumors and 59 non-tumoral thyroid samples. From the whole BC cohort used for *MPPED2* and *DNMT1* expression, a total of 260 primary BC and 61 normal breast surrounding tissues were considered for this study. Patients were classified based on the BC subtype (Lum A, n = 108; Lum B, n = 65; HER2, n = 35; TNBC, n = 52). For the methylation analysis, n = 39 normal tissues and n = 152 primary tumors were examined. *MPPED2-AS1* expression data for BC samples were obtained from TCGA repository (<https://portal.gdc.cancer.gov/repository>), using the same BC cohort utilized for the evaluation of *MPPED2* expression levels. A total of 250 primary BC and 61 normal breast adjacent tissues were considered for this study. Patients were classified based on the BC subtype (Lum A, n = 103; Lum B, n = 62; HER2, n = 35; TNBC, n = 50).

3.6 5-Aza-2'-deoxycytidine (5-Aza-dC) treatment

1×10^5 breast cancer cells were seeded into a 60 mm plate 12 h before treatment. Cells were treated with 5-Aza-20-deoxycytidine (A3656, Sigma-Aldrich) at a concentration of 2 μ M in the growth medium. The growth medium and 5-Aza-dC treatment were refreshed every 24 h for a total of 120 h.

3.7 Amplicon-Based library preparation and targeted bisulfite sequencing

Genomic DNA (1 μ g) was converted by sodium bisulfite treatment with EZ DNA Methylation Kit (Zymo Research, Irvine, CA, USA) according to the manufacturer's instructions. A first amplification step was carried out on bisulfite DNA using the following *MPPED2* specific primers: Forward (Fw) = 5'-aaaTTaatTTaaagtagagaat-3'; Reverse (Rv) = 5'-ctttatAcccacttccaAttac-3'. Capital letters are referred to the C or G after bisulfite treatment. At each primer overhang adaptor sequences were added to obtained:

Fw: 5'-TCGTCGGCAGCGTCAGATGTGTATAAGAGACAG-3'

Rv: 5'-GTCTCGTGGGCTCGGAGATGTGTATAAGAGACAG-3'

The PCR reaction was conducted according to the following conditions: denaturation at 95 °C for 2 min; 35 cycles of denaturation at 95 °C for 30 s, annealing at 52 °C for 40 s, and extension at 72 °C for 50 s. Final elongation at 72 °C was conducted for 6 min. A second PCR step was performed to add Illumina multiplexing indices ("Nextera XT" primers, Illumina, San Diego, CA, USA) that allow samples identification after sequencing. Two purification steps were performed using AMPure magnetic beads (Beckman-Coulter, Brea, CA, USA) following the manufacturer's protocol. After amplicons quantification using Qubit® 2.0 Fluorometer (Life Technologies), an equimolar library of bisulfite-treated amplicons was prepared and then diluted to final concentration of 8 picomolar. To increase diversity in base calling during sequencing, Phix control library was added [8% (v/v)]. Amplicons library was subjected to sequencing using V2 reagents kits on Illumina MiSeq system (Illumina). Paired-end sequencing was performed in 250 cycles per read (250 x 2). An average of 200,000 reads for sample were obtained. For the bioinformatics analyses, paired-end reads were assembled together with a minimum of 40 overlapping residues as threshold with the PEAR tool. FASTQ assembled reads were then converted in FASTA format using the PRINSEQ tool. To analyze the methylation status of each amplicon, we used AmpliMethProfiler pipeline software, a python-based pipeline specifically designed for deep-targeted bisulfite amplicon sequencing. AmpliMethProfiler produces quality filtered FASTA and directly extracts average methylation comparing each sequence with a gene-specific reference file in the FASTA format.

3.8 RNA Immunoprecipitation (RIP) assay

RIP experiments were performed using the Magna RIP™ RNA-Binding Protein Immunoprecipitation Kit (Millipore, Billerica, MA, USA) according to the manufacturer's protocol. Briefly, SKBR3 cells were harvested and lysed in complete RIP lysis buffer. 5 µg of human anti-DNMT1 antibody (#ab13537, Abcam, Cambridge, UK) and normal mouse IgG (Millipore), used as negative control, were incubated with magnetic beads for 30 min. Then, 100 µL of whole lysates were incubated overnight on a rocking platform at 4 °C. Next day, samples were incubated with Proteinase K buffer at 65 °C for 30 min and then immunoprecipitated RNA was purified. Purified RNA was reverse transcribed into cDNA by using random primer with the QuantiTect Reverse Transcription Kit (Qiagen, Hilden, Germany), and analyzed by qRT-PCR.

3.9 Chromatin Immunoprecipitation (ChIP) assay

ChIP experiments were performed in ATC cell lines transiently transfected with *MPED2*-overexpressing vector. Briefly, 48 h after transfection, 5×10^6 SKBR3 cells were cross-linked to fix the DNA-protein complexes using 1% formaldehyde at RT for 10 minutes and the reaction was then stopped by adding

glycine at a final concentration of 0.125 M. Cells were lysed in 300 μ l of buffer containing 10 mM EDTA, 50 mM Tris-HCl pH 8.0, 1% SDS and protease inhibitors and then sonicated three times for 30 cycles (30' ON, 30' OFF) at maximum settings (Bioruptor™ Next Gen, Diagenode Inc., Denville, NJ, USA), obtaining fragments between 0.3 and 1.0 kb. After centrifuging samples at 14000 rpm for 15 minutes at 4°C, 3% of supernatant amount was used as control of the total chromatin obtained (input), and the remaining part of the sample was diluted 2.5-fold in IP buffer (100 mM NaCl, 2 mM EDTA pH 8.0, 20 mM Tris-HCl pH 8.0, 0.5% Triton X-100 and protease inhibitors). After 3 hours of pre-clearing at 4 °C with protein A-Sepharose saturated with salmon sperm (Millipore), samples were mixed overnight at 4 °C with the DNMT1 antibody (#ab13537, Abcam), normal rabbit IgG (sc-2027, Santa Cruz Biotechnology, Dallas, TX, USA). Subsequently, the DNA-protein-antibodies complexes were immunoprecipitated with the proteins A previously used and then the chromatin was released from the beads through 30 minutes incubation with 250 μ l of 1% SDS, 0.1 M NaHCO₃ at 37 °C and finally with 200 nM NaCl at 65 °C overnight. Subsequently, 10 μ l of 0.5 mM EDTA, 20 μ l of 1 M Tris-HCl pH 6.5 and 20 μ g of Proteinase K were added to the reaction tube and then the complexes were incubated for 1 hour at 45 °C. DNA from chromatin immunoprecipitated was purified by phenol/chloroform extraction (Life Technologies) and precipitated by adding two volumes of ethanol and 0.1 M CH₃COONa. IgG was used as non-specific control and input DNA values were used to normalize the values from qChIP samples. The percentage of IP chromatin was calculated as $2^{-\Delta Ct} \times 3$, where ΔCt is the difference between Ct (input) and Ct (IPsample), and 3 is the percentage of the total sample used for the input. The relative abundance of immunoprecipitated chromatin was expressed as the percentage of binding of interested promoter compared to the input. The ChIP was carried out with the following primer:

MPPED2 promoter Fw: 5'-CGGGTGTTCGTAGTGTGGA-3'

MPPED2 promoter Rv: 5'-AAACGATACCCACACGCCTT-3'

3.10 Immunohistochemical evaluation of a breast tissue microarray (TMA)

A human breast cancer TMA was purchased from Super Bio Chips (Super Bio Chips Laboratories, Seoul, Korea). TMA section was deparaffinized in xylene (2x 10 minutes) and re-hydrated in ethanol solutions at decreasing concentration (from 100% to 50%). TMA slide was then permeabilized in PBS-0.2% triton (5 minutes), washed 2x 5 minutes with PBS and, subsequently, it underwent unmasking treatment in citrate buffer (0.01 M pH6) for 15 minutes in microwave. Endogenous peroxidases were then blocked with methanol and 1.5% oxygen peroxide and tissues were once again permeabilized with PBS-0.2% triton for 5 minutes, washed 2x 5 minutes in PBS and blocked in blocking solution (5% normal goat serum, 3% BSA, 20 mM MgCl₂, 0.3% tween 20 in PBS) for 1 hour at RT. The rabbit polyclonal MPPED2 antibody (H00000744-D01P, Abnova, Taipei City,

Taiwan) was used 1:50 in blocking solution overnight at 4°C. The section then underwent to the following protocol: PBS-0.2% triton for 5 minutes, PBS 2x 5 minutes, 1 hour biotinylated α -rabbit IgG, H+L secondary antibody (BA-1000, Vector Laboratories, Burlingame, USA) 1:100 in blocking solution for 1 hour at RT, PBS-0.2% triton for 5 minutes, PBS 2x 5 minutes, ABC (SK-4000, Vector Laboratories) for 30 minutes at RT, PBS-0.2% triton for 5 minutes, PBS 3x 5 minutes, DAB substrate (SK-4100, Vector Laboratories). The slide was then dehydrated and covered with glass using D. P. X. mountant liquid (GRM655, Sigma-Aldrich) and finally acquired with a NanoZoomer Digital Pathology System (Hamamatsu, Shizuoka, Japan). TMA comprised n=59 total cases including, n=40 primary tumor samples, n=10 metastatic samples, and n=9 normal adjacent tissues. However, only n=54 samples, including n=38 primary tumors, n=10 metastases, n=6 normal adjacent tissues were evaluable. Two pathologists evaluated slide independently. For each tissue spot, the intensity of the staining and the percentage of positive cells were recorded. The intensity of the staining was scored from 0 to 3+, where 0 is no staining, 1+ is weak staining, 2+ is moderate staining and 3+ is strong staining. H-score was calculated according to the following formula: 1x (% of 1+ cells) +2x (% of 2+ cells) +3x (% of 3+ cells), to assign to each sample an expression value based on the percentage of MPPED2 expressing cells and the intensity of staining.

3.11 RNA extraction and quantitative Real-Time PCR (qRT-PCR)

Total RNA from thyroid and breast tissues and cell lines was extracted using Trizol reagent (Life Technologies). 1 μ g of total RNA from each sample was used to obtain double-strand cDNA with the QuantiTect Reverse Transcription Kit (Qiagen). Quantitative Real-Time PCR (qRT-PCR) was performed with the CFX96 thermocycler (Bio-Rad, Hercules, CA, USA) in 96-well plates. For each PCR reaction, 10 μ l of 2x Sybr Green (Bio-Rad), 200 nM of each primer and 20 ng of the cDNA, previously generated, were used. The oligonucleotides for qRT-PCR, encompassing exon-exon junctions, were purchased from Integrated DNA Technologies (San Diego, CA, USA) and designed with Primer-BLAST software. Sequences are as follows:

MPPED2:

Fw: 5'-GCTTCAAAGAGTGGGCTGTG-3',

Rv: 5'-GAGGGTTGGTCGGTTGAAAG-3'

RP18S:

Fw: 5'-TGCGAGTACTCAACACCAA-3',

Rv: 5'-TTGGTGAGGTCAATGTCTGC-3'

MPPED2-AS1:

Fw: 5'-TGGTGCAGGGATTGTTGCAT-3',

Rv: 5'-TGAACGACTGCAACTGCTTTG-3'.

Relative gene expression was determined using comparative C(T) method, as described elsewhere. RP18S was used as housekeeping gene.

3.12 Western blot

Cells were homogenized in RIPA lysis buffer (20 mM Tris-HCl pH 7.5, 5 mM EDTA, 150 mM NaCl, 1% Nonidet P40, and a mix of protease inhibitors). Cell protein lysates were then subjected to SDS/PAGE and transferred onto Immobilon-P transfer membranes (Merck, Burlington, MA, USA). Membranes were blocked with 5% non-fat milk and probed with the indicated antibodies at the appropriate dilutions: MPPED2 (1:500; NBP1-80499, Novus Biologicals, Centennial, CO, USA), cyclin D1 (1:1000; sc-718, Santa Cruz Biotechnology), cyclin E (1:1000; sc-248, Santa Cruz Biotechnology), ZEB1 (D80D3) (1:500, #3396S, Cell Signaling, Danvers, MA, USA), E-cadherin (24E10) (1:500; #3195, Cell Signaling), β -actin (1:5000; A5441, Sigma-Aldrich) and α -tubulin (1:10000; T6074, Sigma-Aldrich). Membranes were incubated with horseradish peroxidase-conjugated secondary antibody (1:3000) for 60 minutes at RT. Signals were finally detected with chemiluminescent detection system (ECL) (Thermo Fisher Scientific, Waltham, MA, USA), and films were developed with a semiautomatic developing machine (Cawomat IR 2000, CAWO Photochemisches, Schrobenhausen, Germany). Densitometric analyses of the Western blot bands were evaluated by using ImageJ 1.43 software.

3.13 Flow cytometry

For flow cytometry analyses breast cancer cells were seeded into a 100 mm plate, were trypsinized, washed twice in cold PBS and fixed with 70% ethanol, after 96 hours. After centrifugation at 1,200 rpm for 10 minutes at 4 °C, cells were treated with 50 μ g/ml propidium iodide and 25 μ g/ml RNase DNase-free (Roche, Basel, Switzerland) in PBS for 20 minutes at RT, safe of light. For each measurement 10,000 events were analyzed by employing a BD AccuriTM C6 flow cytometer (BD Biosciences, Franklin Lakes, NJ, USA) and cell cycle data were analyzed with the BD Accuri C6 Software in a semiautomatic analysis procedure.

3.14 Cell migration and invasion assays

Migration and invasion assays were performed using a transwell chamber (8 μ m pores). The invasion was estimated by using Matrigel (BD Biosciences). Briefly, cells (3×10^4 for migration and 1×10^5 for invasion) were plated in the upper transwell chamber in serum-free medium. Then, 0.3 ml complete medium was added in the lower chamber as a chemoattractant. After 24 hours (migration) and 48 hours (invasion) of incubation, migrated or invaded cells on the membrane of the chambers were fixed and stained with crystal violet solution (crystal violet 0.05%, methanol 20%). After acquisition of images, crystal violet in the chamber was de-stained with PBS-0.1% SDS solution and was read at 590 nm in a microplate reader (LX800, Universal Microplate Reader, BioTek Instruments, Inc., Winooski, VT, USA). Cancer cell lines were also seeded in a 96 well plate to normalize the number of used cells. After two hours, the absorbance at 490 nm was read using

cell titer (Promega, Fitchburg, WI, USA). Results were obtained by normalizing the crystal violet values to cell titer ones.

3.15 Colony formation assay

MDA-MB-231 and SKBR3 cells at 80% of confluency in 100 mm plate were transfected with pCDNA3.1-EV and pCDNA3.1-MPPED2. 24 hours after transfection, cells were treated with 600 $\mu\text{g/ml}$ and 100 $\mu\text{g/ml}$ hygromycin, respectively. Medium containing hygromycin was refreshed every two days and, after 3 weeks of hygromycin selection, cells were fixed and stained with a solution containing crystal violet.

3.16 Growth curve assay

For growth curve assay, 2×10^4 thyroid cancer cells and 3×10^4 breast cancer cells were plated in a 60 mm plate. Cells were counted in triplicate with Burker hemocytometer chamber to evaluate cell growth rate for 5 days.

3.17 Statistical analysis

All results were reported as mean \pm standard deviation (SD). Data were analyzed by Student's t-test, Mann Whitney's test and Anova test, when required. The correlations were evaluated through non-parametric Spearman's Rank correlation coefficient with 95% confidence interval. To assess the relationship between protein expression levels and clinicopathological features, Fisher's exact test was used. Statistical analyses were carried out using GraphPad Prism software 6.0 and the difference was considered significant when $p < 0.05$.

4. Results

4.1 Identification of lncRNAs deregulated in PTC

In order to identify new molecules and pathways involved in thyroid carcinogenesis, the expression signature of lncRNAs in twelve PTC and four normal thyroid tissues was analyzed through a Human lncRNA Microarray Version 3.0 (Arraystar, Rockville, MD, USA). This analysis revealed 1560 deregulated lncRNAs (DELncRNAs) in PTC tissues (fold change >2 and p -value<0.05), including 345 up- and 1215 downregulated lncRNAs in comparison with normal thyroid ones. Due to the large number of DELncRNAs obtained from this analysis, we decided to improve the power of the microarray data by using false discovery rate (FDR)≤0.01 and p -value<0.001 filtering. By these procedures, we obtained 56 statistical DELncRNAs, including 12 high- and 44 low-expressed lncRNAs in PTCs (Figure 9). In Table 4 are shown the most significant up- and downregulated lncRNAs, classified based on the intersection with protein-coding genes in intergenic, intronic antisense position, natural antisense, and bidirectional.

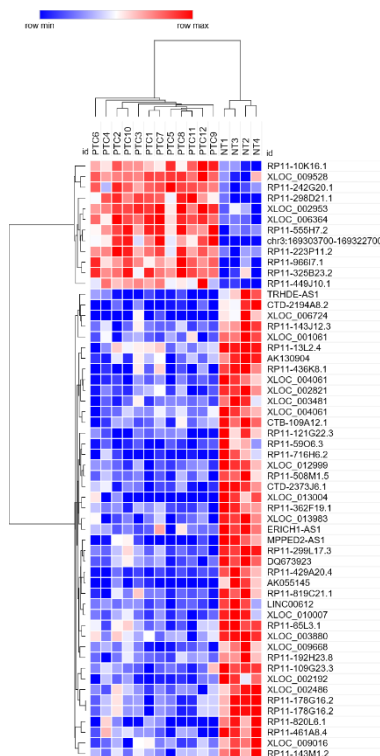


Figure 9. lncRNAs signature in PTC samples and normal thyroid tissues. Heat map with the expression levels of 56 significantly altered lncRNAs (row) (p <0.001 and FDR≤0.01) in twelve papillary thyroid carcinoma and four non-tumoral thyroid tissues. Hierarchical clustering among the 56 DELncRNAs is also showed. Each cube is color-coded by sample normalized intensity ranging from blue (low intensity) through white to red (high intensity).

Table 4. Representative list of deregulated lncRNA in PTC vs NT

Gene Symbol	FC	p-Value	FDR	Relationship	Associated genes
<i>XLOC_002953</i>	3.31342	1.09×10^{-05}	0.0072592	intergenic	
<i>RP11-10K16.1</i>	3.12298	3.15×10^{-05}	0.0097872	natural antisense	
<i>RP11-555H7.2</i>	2.68946	1.78×10^{-05}	0.0082546	intergenic	GALN7
<i>RP11-298D21.1</i>	2.65662	4.29×10^{-06}	0.0037156	intronic antisense	
<i>RP11-966I7.1</i>	2.64687	2.74×10^{-06}	0.0030284	bidirectional	CDH13
<i>XLOC_009528</i>	2.51675	1.64×10^{-05}	0.0082375	intergenic	FOXG1
<i>XLOC_006364</i>	2.49504	1.39×10^{-06}	0.0029014	intergenic	
<i>RP11-242G20.1</i>	2.37511	6.10×10^{-06}	0.0045054	intergenic	
<i>RP11-325B23.2</i>	2.31346	2.29×10^{-05}	0.0087685	intronic antisense	OR5K4
<i>RP11-449J10.1</i>	2.26852	2.40×10^{-05}	0.0087685	intronic antisense	ADAMTS18
Gene Symbol	FC	p-Value	FDR	Relationship	Associated genes
<i>RP11-429A20.4</i>	19.714	1.90×10^{-09}	3.79×10^{-05}	intergenic	
<i>XLOC_004061</i>	19.208	2.48×10^{-07}	0.0012331	intergenic	
<i>RP11-299L17.3</i>	18.817	5.37×10^{-07}	0.0021199	intergenic	
<i>RP11-59O6.3</i>	10.338	2.42×10^{-05}	0.0087684	intronic antisense	DOCK8
<i>MPPED2-AS1</i>	10.2854	7.45×10^{-06}	0.005301	intronic antisense	MPPED2
<i>TRHDE-AS1</i>	10.2272	3.81×10^{-06}	0.0036155	intronic antisense	TRHDE
<i>CTD-2194A8.2</i>	9.10460	2.45×10^{-06}	0.0029312	intronic antisense	ACSM5
<i>RP11-121G22.3</i>	8.72347	5.89×10^{-06}	0.0045054	intronic antisense	PPFIA2
<i>RP11-436K8.1</i>	8.37078	1.76×10^{-05}	0.0082546	intergenic	
<i>RP11-109G23.3</i>	7.919314	1.74×10^{-06}	0.0029312	bidirectional	

FC, fold change; FDR, False Discovery Rate

It is well demonstrated that intronic antisense lncRNAs (localized in antisense position to the direction of transcription of the host protein-coding genes) can modulate the expression of their associate gene (Kotake *et al.*, 2011, Yap *et al.*, 2010). Given this consideration, we focused our attention on the intronic antisense class of lncRNAs. Among them, we observed that the lncRNA *MPPED2 antisense RNA1* (*MPPED2-AS1*, previously known as *RP5-1024C24.1*), was strongly and significantly downregulated in PTC samples. Importantly, through bioinformatic analysis, we observed that this lncRNA is located on chromosome 11 and transcribed in the opposite direction to *MPPED2* gene, which encodes a metallophosphoesterase protein, already reported to be downregulated and to play an important anti-oncogenic role in several neoplasia as oral squamous cell carcinoma (Shen *et al.*, 2016), cervical cancer (Zhang *et al.*, 2016) and neuroblastoma (Liguori *et al.*, 2012). Consequently, by using data available in the The Cancer Genome Atlas (TCGA) database, we observed that also *MPPED2* was strongly and significantly downregulated in TC tissues (Figure 10), leading us to suppose its implication in this type of tumor, and therefore, encouraging to study in depth the *MPPED2-AS1* and *MPPED2* role and their possible relationship in TC.

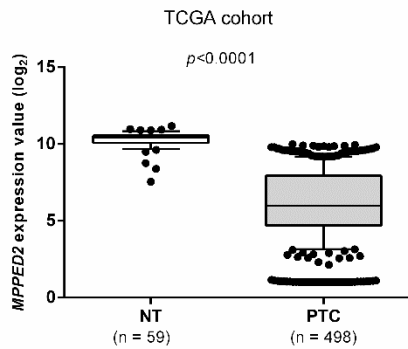


Figure 10: Analysis of *MPPED2* expression in thyroid carcinomas (TCGA). *MPPED2* expression levels were evaluated in a dataset available in TCGA comprising 59 normal thyroid (NT) and 498 papillary thyroid cancers (PTC); $p < 0.0001$.

Consequently, to uncover their contribution in thyroid carcinogenesis, we assessed *MPPED2AS1* and *MPPED2* expression levels in a set of 23 PTC samples by qRT-PCR. In Figure 11A and 11B, a strong reduction of both genes was observed in all PTC specimens when compared to the normal thyroid ones, confirming their reduction in the well differentiated TC. Subsequently, their expression levels were assessed in a set of thyroid neoplasms, including 9 follicular adenomas (FTAs), additional 11 PTCs, 5 FTCs and 11 ATCs and compared with non-tumoral thyroid tissues. Interestingly, we observed that their expression levels gradually decreased going from benign TCs to well-differentiate TCs and to undifferentiated ones (Figure 11C and 11D). Then, we observed a significant correlation between *MPPED2-AS1* and *MPPED2* expression in the whole set of TC histotypes ($r = 0.5604$; $p < 0.001$), suggesting that *MPPED2-AS1* and *MPPED2* are co-regulated during the process of thyroid carcinogenesis (Figure 11E).

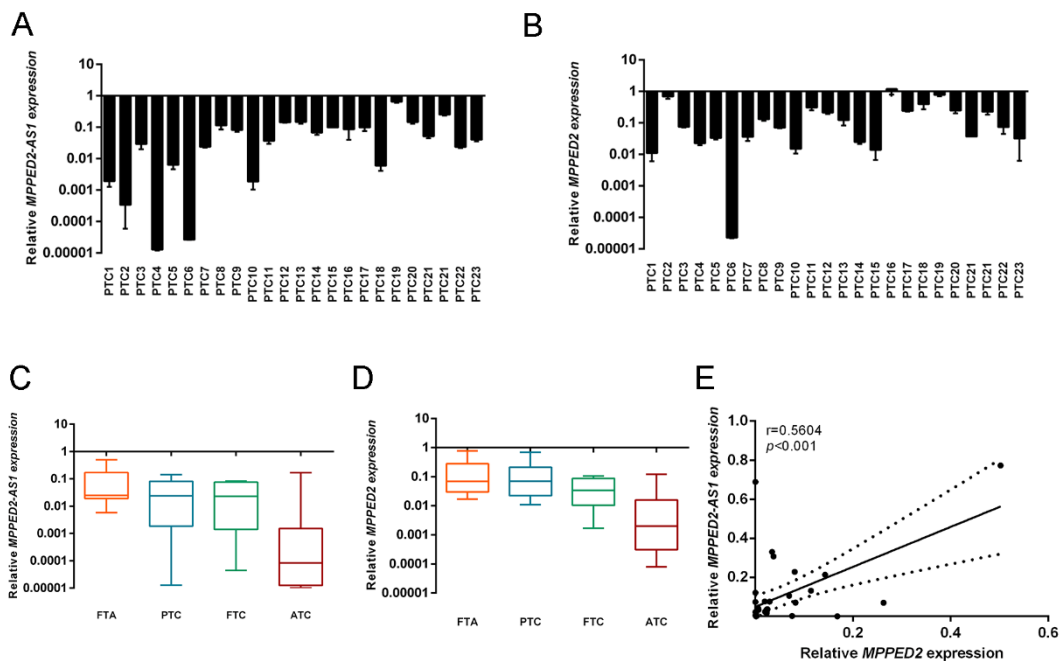


Figure 11. Analysis of *MPPED2-AS1* and *MPPED2* expression in human TC tissues. (A,B) *MPPED2-AS1* and *MPPED2* expression levels were evaluated by qRT-PCR in 23 PTC. Data are reported as $2^{-\Delta\Delta Ct}$ values \pm SD, compared to the mean of thyroid normal tissues, set equal to 1. (C,D) *MPPED2-AS1* and *MPPED2* levels were analyzed by qRT-PCR in a set of TC samples (FTA, n=9, PTC, n=11; FTC, n=6; ATC, n=11). Data are reported as $2^{-\Delta\Delta Ct}$ values \pm SD, compared to the mean of thyroid normal tissues, set equal to 1. (E) Correlation scatter plot (Spearman's Rank) between qRT-PCR levels of *MPPED2* and *MPPED2-AS1* analyzed in thyroid carcinoma samples ($r=0.5604$; $p<0.001$).

4.2 *MPPED2* is induced by *MPPED2-AS1* and their restoration negatively modulates cell proliferation and migration of thyroid cancer cells

To define the role of *MPPED2-AS1* and *MPPED2* in thyroid carcinogenesis, we modulate their expression in TC cell lines. To achieve this aim, we analyzed *MPPED2-AS1* and *MPPED2* expression in a panel of thyroid carcinoma cell lines, including TPC-1 and B-CPAP (PTC-derived cell lines), WRO (FTC-derived cell line) and FB-1 and FRO (ATC-derived cell lines) by qRT-PCR. As shown in Figure 12, the expression of *MPPED2-AS1* and *MPPED2* was extremely lower in all TC cell analysed in comparison with three normal thyroid samples used as control.

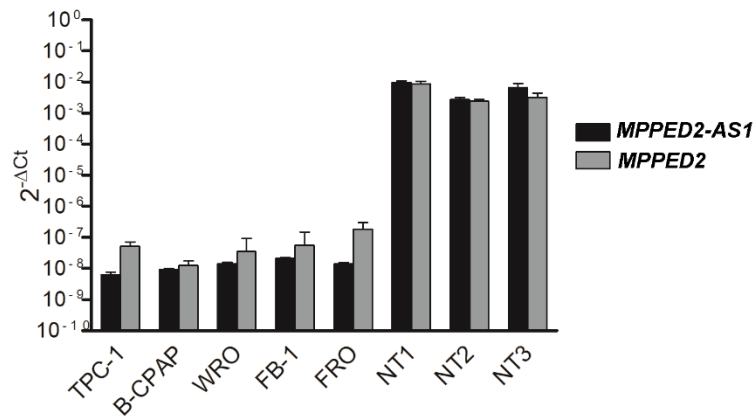


Figure 12. Expression analysis of *MPPED2AS1* and *MPPED2* in TC cell lines. qRT-PCR performed on papillary (TPC-1, B-CPAP), follicular (WRO), anaplastic (FB-1 and FRO) TC cell lines and three normal thyroid tissue samples (NT1, NT2, NT3). Data are reported as $2^{-\Delta Ct}$ values \pm SD.

Subsequently, we decided to stably restore their expression in TPC-1 and FRO TC cell systems to carry out functional analysis. In Figure 13A and 13B is shown the increased expression of *MPPED2-AS1* levels by qRT-PCR, whereas in Figure 13C and 13D is reported the high levels of *MPPED2* through qRT-PCR and Western blot analyses in both TPC-1 and FRO cell lines. After the stable restoration of their expression, we evaluated their functional effects in order to unveil their role in TC. As given in Figure 13E and 13F, the growth curve assays showed that both the TPC-1-*MPPED2-AS1* and FRO-*MPPED2-AS1* cells exhibited a lower proliferation rate than cells carrying the empty vector (EV). Similar results were

obtained in TPC-1-*MPPED2* and FRO-*MPPED2*, which displayed a significant reduction in the cell growth rate compared to the respective EV transfected cells (Figure 13G and 13H). These results demonstrated that both genes are able to negatively modulate cell proliferation in TC cell lines.

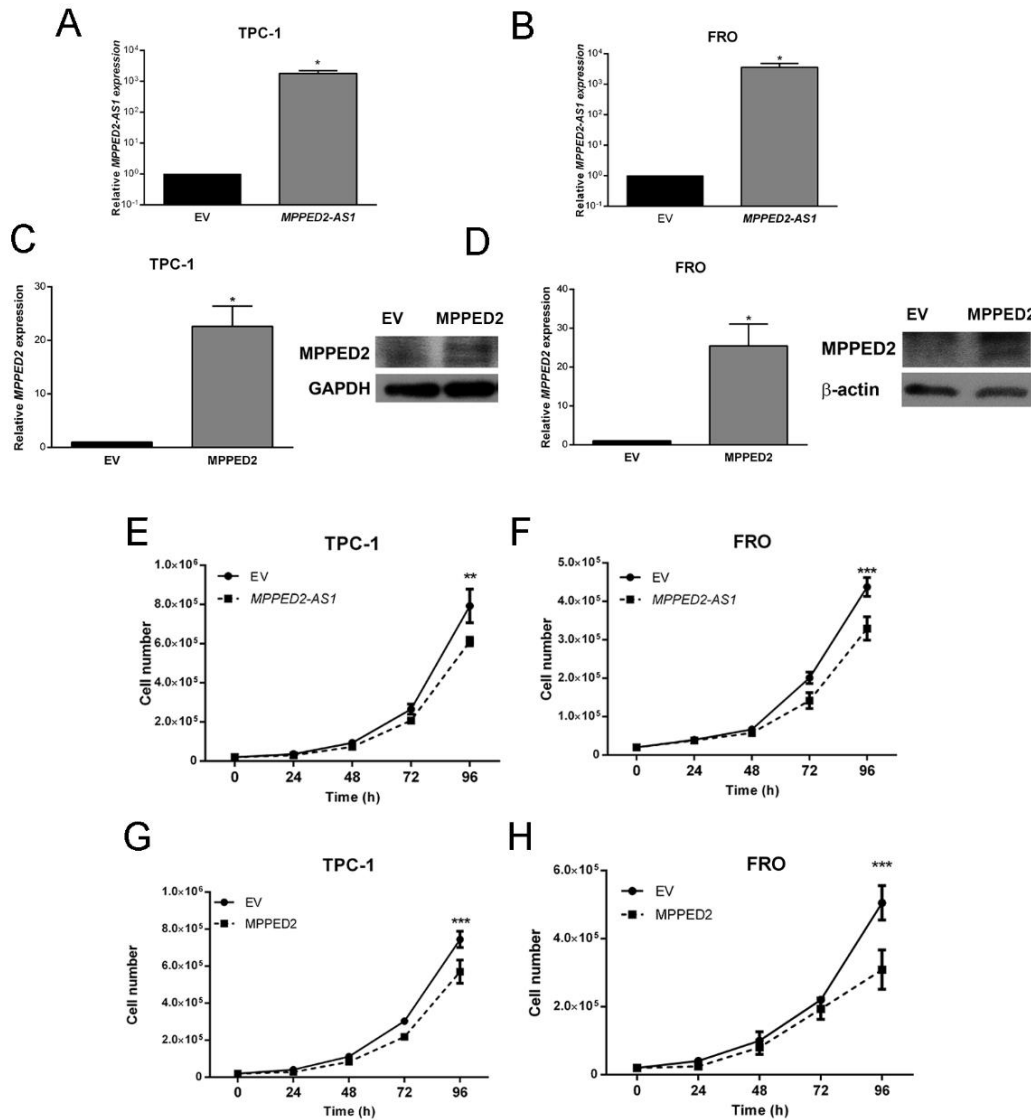


Figure 13. *MPPED2-AS1* and *MPPED2* decreases cell proliferation of TC cell lines. (A,B) qRT-PCR analysis performed on TPC-1 and FRO cell lines stably carrying *MPPED2-AS1* or the corresponding empty vector (EV). Results were obtained from four independent experiments. Data are reported as $2^{-\Delta\Delta C_t}$ values \pm and were compared to EV, set equal to 1. t-test; $p < 0.05$. (C,D) qRT-PCR analysis performed on TPC-1 and FRO cell lines stably carrying *MPPED2* or the corresponding EV. Data are reported as $2^{-\Delta\Delta C_t}$ values \pm SD and were compared to EV, set equal to 1. t-test; $p < 0.05$. Immunoblot analysis confirming the expression of *MPPED2*. GAPDH and β -actin were used to normalize the amount of loaded protein. (E,F) Cell growth analysis of TPC-1 and FRO stably carrying *MPPED2-AS1* or EV. Cell number was evaluated at 24 h, 48 h, 72 h and 96 h after seeding. Values were obtained from three independent experiments. Data were reported as mean \pm SD. 2-way Anova-test; $p < 0.01$. (G,H) Cell growth analysis of TPC-1 and FRO stably carrying *MPPED2* or

EV. Cell number was evaluated at 24 h, 48 h, 72 h and 96 h after seeding. Values were obtained from three independent experiments and data were reported as mean \pm SD. 2-way Anova-test: $p < 0.001$.

Subsequently, to evaluate their effects on TC progression we performed transwell assays on TC cell lines overexpressing *MPPED2-AS1* and *MPPED2*. Interestingly, a significant reduction of migration in TC cells stably expressing *MPPED2-AS1* (Figure 14A) and *MPPED2* (Figure 14B) was detected when compared to the respective controls. These findings demonstrate their inhibiting role in cellular migration and, thus, indicate their involvement in cancer-malignant processes.

Intronic antisense lncRNAs usually acts through the modulation of the host protein-coding genes expression. Therefore, we investigate whether *MPPED-AS1* is involved in such mechanism. Consequently, *MPPED2* expression was evaluated in TPC-1 and FRO stably expressing *MPPED-AS1* by qRT-PCR. Intriguingly, we found that the lncRNA is able to increase the expression of *MPPED2* in such cell lines with respect to the EV transfected cells (Figure 14C and 14D), indicating that the lncRNA may act through the modulation of the *MPPED2* expression.

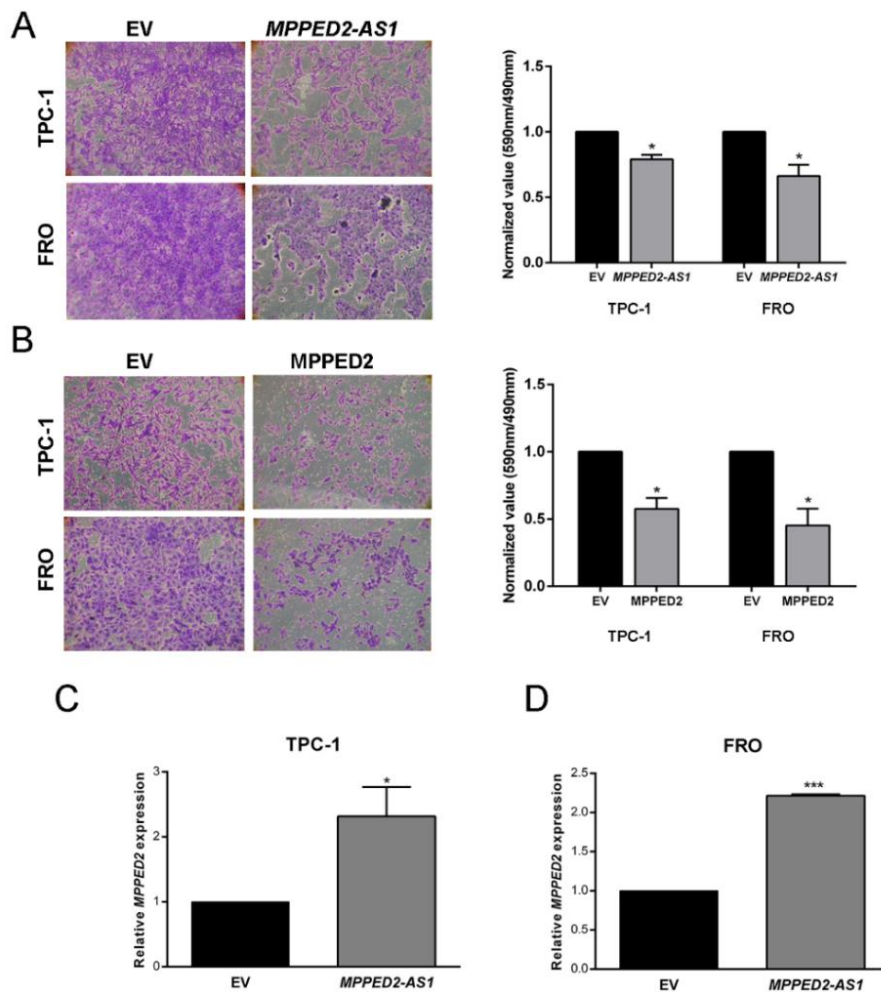


Figure 14. *MPPED2-AS1* and *MPPED2* delay the migration of TC cells. (A,B) Representative acquisition of migration assays performed on TPC-1 and FRO stably carrying *MPPED2-AS1* or *MPPED2* and the corresponding EV. Magnification 40 x. (left panel). Data obtained from three independent experiments are shown in the right panel. Values were reported as mean value \pm SD and compared to the EV, set equal to 1. t-test; $p < 0.05$. (C,D) *MPPED2* expression evaluated by qRT-PCR in TPC-1 and FRO stably expressing *MPPED2-AS1*. Data were obtained from three independent experiments. Values were reported as relative expression \pm SD and were compared to the EV, set equal to 1. t-test; $p < 0.05$; $p < 0.001$.

4.3 *MPPED2-AS1* and *MPPED2* are downregulated in human breast cancer samples

Since the mechanisms of action of the identified *MPPED2-AS1* and *MPPED2* genes could represent a more general events not only specific of thyroid carcinogenesis, we extended the expression analysis to additional cancer types deriving from different anatomic districts. Therefore, preliminary analysis with the

data available in the TCGA dataset reported that *MPPED2-AS1* and *MPPED2* expression decreases in BC, colon adenocarcinomas and lung adenocarcinoma respect the non-tumoral counterpart, even though their reduction appears to be more specific for BC one. Consequently, we decided to unveil their role in BC aiming also to identify new players in breast carcinogenesis. To achieve this aim, we extended our expression analysis in a set of 45 human BC samples. The results reported in Figure 15A, clearly confirmed the reduction of *MPPED2* in such BC specimens in comparison with the normal breast tissues by qRT-PCR ($p=0.0027$). Subsequently, *MPPED2* levels were also analyzed using data available in the TCGA BC database, in a cohort comprising 260 BC samples and 61 breast normal tissues. As expected, even in this cohort, *MPPED2* expression has been found significantly lower in 260 primary BC samples in comparison with normal breast tissues ($p<0.0001$) (Figure 15B), confirming once more its strongly reduction. Also, its expression was assessed by qRT-PCR in a panel of BC-derived cell lines, including MCF7 (Lum A), BT-474 (Lum B), SKBR3 (HER2) and MDA-MB-231 (TNBC), and extremely low expression levels of *MPPED2* were found, particularly in SKBR3 and MDA-MB-231 BC cells (Figure 15C). Finally, *MPPED2* expression was also examined in the different BC molecular subtypes (Lum A, Lum B, HER2, and TNBC) of the TCGA BC cohort, and a significant *MPPED2* reduction has been observed in all the analyzed subtypes ($p<0.0001$), particularly in HER2 and in TNBC ones (Figure 15D). Specifically, *MPPED2* was found even lower in ER- BC samples respect to ER+ ones (Figure 15E), indicating that *MPPED2* downregulation is related to BC progression.

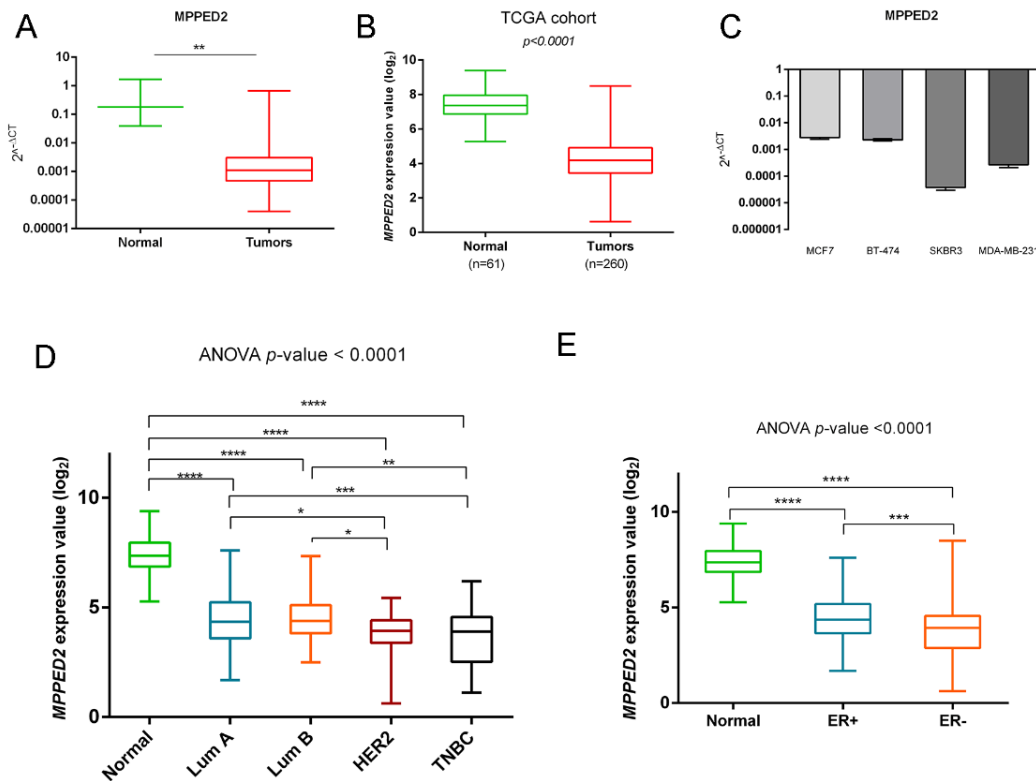


Figure 15. Expression of *MPPED2* in human breast carcinoma tissues. (A) *MPPED2* expression levels were evaluated by qRT-PCR in 45 breast carcinoma tissues. Data are reported as $2^{-\Delta\Delta C_t}$ values \pm SD, compared to the mean of breast normal tissues, set equal to 1. *t*-test: $p < 0.0027$ (B) *MPPED2* expression levels were evaluated in a dataset available in TCGA; $p < 0.0001$. (C) *MPPED2* mRNA levels were assessed in a panel of human breast carcinoma cell lines by qRT-PCR. Data are reported as $2^{-\Delta C_t}$ values \pm SD. (D) *MPPED2* expression levels were evaluated in the molecular subtypes of breast carcinoma tissues in the TCGA dataset. Box and whiskers: min to max. One-way Anova test: $p < 0.0001$. (E) *MPPED2* expression levels were evaluated in the TCGA dataset. ER+ ($n = 172$), ER- ($n = 88$) and normal ($n = 61$) breast samples were evaluated. Box and whiskers: min to max. One-way Anova test: $p < 0.0001$; $p < 0.001$.

Subsequently, *MPPED2-AS1* expression was also examined by qRT-PCR in the same panel of human BC samples used for *MPPED2*. Like *MPPED2*, the *MPPED2-AS1* levels were found significantly lower in the BC samples analyzed, ($p = 0.0199$) (Figure 16A). Additionally, the lncRNA levels were also examined by qRT-PCR in the panel of BC-derived cell lines. Similar to *MPPED2*, extremely low levels of *MPPED2-AS1* were observed even in the whole set of BC cell system (Figure 16B). Moreover, using the same TCGA BC cohort, the reduction of *MPPED2-AS1* was confirmed in the BC samples analyzed compared to the normal breast tissues ($p < 0.0001$) (Figure 16C), even though for many samples *MPPED2-AS1* expression was not detectable and, thereby, any significant difference was found among the different BC subtypes (Figure 16D). After that, a correlation between *MPPED2-AS1* and *MPPED2* expression was evaluated, and a significant

positive one was found ($r=0.6646$; $p<0.0001$) (Figure 16E), indicating that the co-regulation of *MPPED2* and *MPPED2-AS1* genes also occurs in BC.

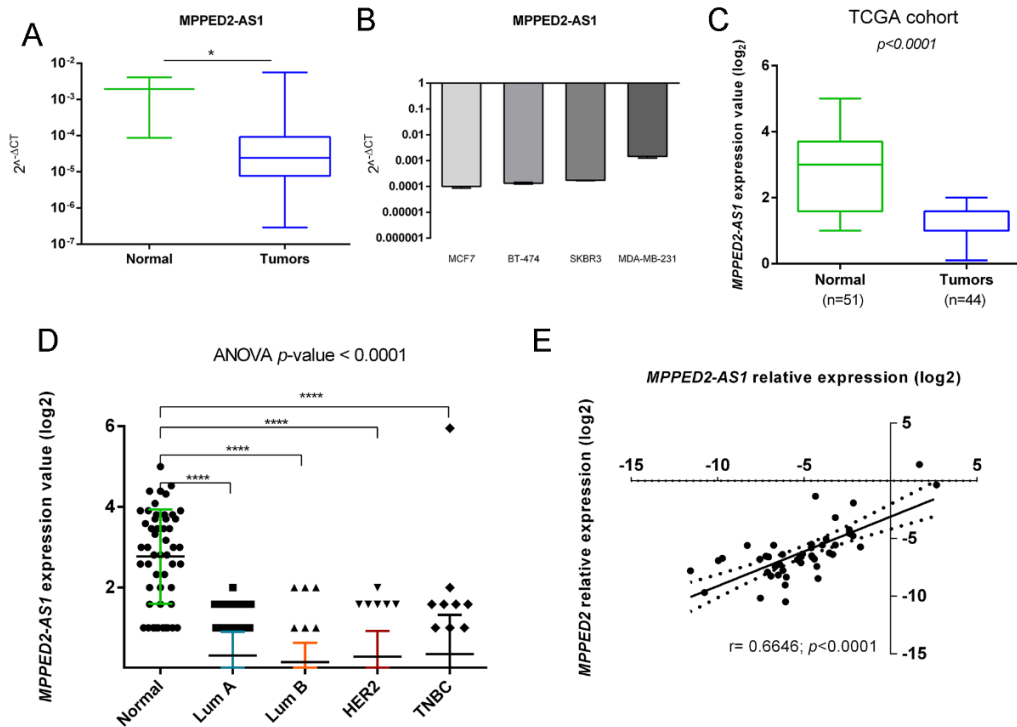


Figure 16. Expression of *MPPED2-AS1* in human breast carcinoma tissues. (A) *MPPED2-AS1* levels were evaluated in 45 breast carcinoma tissues by qRT-PCR. Data are reported as $2^{-\Delta\Delta C_t}$ values \pm SD, compared to the mean of breast normal tissues, set equal to 1. t -test: $p=0.0199$ (B) *MPPED2-AS1* mRNA levels were evaluated in a panel of human breast carcinoma cell lines by qRT-PCR. Data are reported as $2^{-\Delta C_t}$ values \pm SD (C) *MPPED2-AS1* expression levels were evaluated in the TCGA dataset. t -test: $p<0.0001$. (D) *MPPED2* expression levels were evaluated in the molecular subtypes of breast carcinoma tissues in the TCGA dataset. One-way Anova test: $p<0.0001$. (E) Correlation scatter plot (Spearman's Rank) between qRT-PCR levels of *MPPED2* and *MPPED2-AS1* analyzed in 45 breast carcinoma samples ($r=0.6646$; $p<0.0001$).

Further, *MPPED2* protein expression was also evaluated by immunohistochemical (IHC) staining in a tissue microarray (TMA) containing 38 primary BC tissues, 10 metastases, and 6 normal adjacent breast tissues, using a specific antibody against *MPPED2*. The view of IHC staining of the TMA slide is shown in Figure 17A, and the results of the IHC were summarized in Table 5. Representative results showed a weak *MPPED2* staining in matched primary BC samples (score = 2+; score = 1+) and metastases (score = 2+; score = 1+) when compared to the normal adjacent tissues (score = 3+) (Figure 17B). For each spot, H-score was obtained combining the percentage of positive cells with the intensity

score. H-score results confirmed the reduction of MPPED2 in tumor tissues ($p<0.001$) and metastases ($p<0.01$), in comparison with the normal adjacent breast tissues (Figure 17C). Instead, statistical IHC analysis reveals no significant association between MPPED2 expression and BC feature as tumor size, histological grade, lymph node, TNM stage and the status of ER, PR, and HER2, while a significant one was found with age ($p=0.0002$) (Table 6).

Table 5. MPPED2 protein expression evaluated by immunohistochemistry

Histological type	MPPED2 staining score ^a, n (%)			
	0	1+	2+	3+
Normal adjacent tissues (n=6)	0 (0)	0 (0)	0 (0)	6 (100)
Primary BC tissue (n=38)	3 (7.8)	10 (26.3)	12 (31.5)	13 (34.2)
BC metastatic carcinoma (n=10)	0 (0)	3 (30)	4 (40)	3 (30)

^a 0, no signal; 1+, weak signal; 2+, moderate signal; 3+, strong signal.

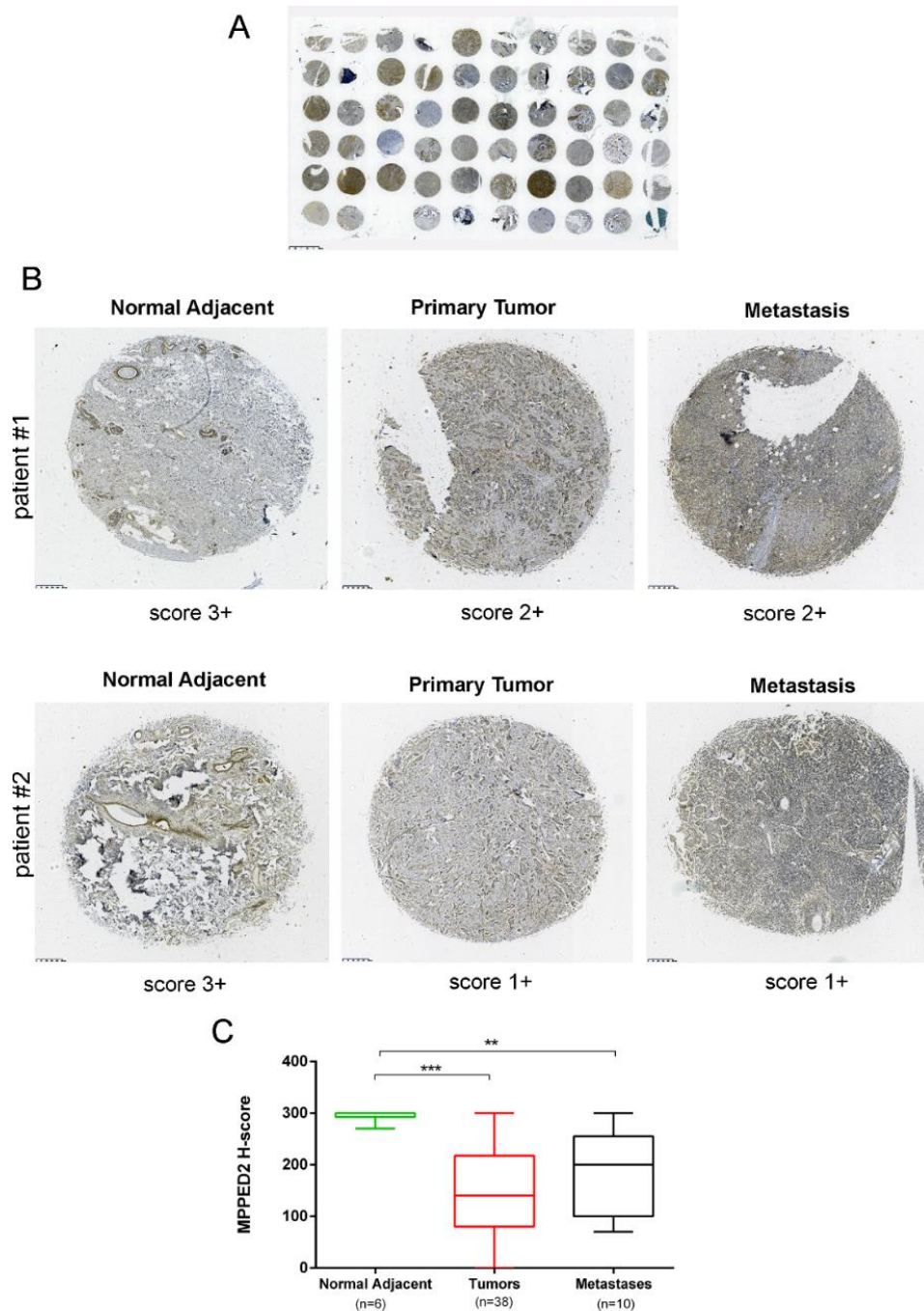


Figure 17. MPPED2 protein expression in human breast carcinoma tissues. (A) Gross view of immunohistochemical staining of a tissue microarray (TMA) slide. Scale bar, 2.5 mm. (B) Representative immunohistochemical staining of MPPED2 protein in normal adjacent tissue (left), breast primary tumor (center) and metastatic tissue (right) derived from two different patients, respectively. MPPED2 signal is strong in normal adjacent tissue (score 3+) and moderate (score 2+) or weak (score 1+) in the primary tumor or metastatic tissues (magnification 200 \times). Scale bar, 250 μ m. (C) Intensity of the staining and the percentage of positive cells were combined to obtain H-score. Box and whiskers: min to max; Mann Whitney test: $p < 0.001$; $p < 0.01$; ns, not significant.

Table 6. Association of MPPED2 expression and tissue microarray (TMA) breast cancer characteristic.

Characteristic	n	MPPED2 Staining		p-Value*
		Low (0,1+) n (%)	High (2+,3+) n (%)	
<i>Age</i>				
<50	22	12 (31.6)	10 (26.3)	0.0002
≥50	16	1 (2.6)	15 (39.5)	
<i>Tumor size</i>				
≤3 cm	16	5 (13.2)	12 (31.6)	0.734
>3 cm	22	8 (21)	13 (34.2)	
<i>Nottingham histological grade</i>				
I	0			0.968
II	16	6 (15.8)	10 (26.3)	
III	19	7 (18.4)	12 (31.6)	
NA	3		3 (7.9)	
<i>Lymph node</i>				
Negative	13	3 (7.9)	10 (26.3)	0.473
Positive	25	10 (26.3)	15 (39.5)	
<i>Estrogen receptor</i>				
Negative	27	11 (28.9)	16 (42.1)	0.267
Positive	11	2 (5.3)	9 (23.7)	
<i>Progesterone receptor</i>				
Negative	28	11 (29)	17 (44.7)	0.441
Positive	10	2 (5.3)	8 (21)	
<i>Her2</i>				
Negative	28	9 (23.7)	19 (50)	0.709
Positive	10	4 (10.5)	6 (15.8)	
<i>Tumor stage</i>				
I	0			0.295
II	23	6 (15.8)	17 (44.7)	
III	15	7 (18.4)	8 (21)	
Total	38			

* Fisher's exact test: samples were grouped in low (0, 1+) and high (2+, 3+) expressors, based on the intensity of the staining. NA, not available.

4.4 MPPED2 promoter is hypermethylated in human breast cancer samples

To define the mechanism that leads to MPPED2 reduction in BC, the methylation of a CpG island upstream the transcriptional start site (TSS) of the *MPPED2* gene was evaluated by performing next-generation sequencing on 16 matched DNAs derived from normal and BC tissues, after bisulfite treatment. Intriguingly, the obtained results showed that the CpG island, comprising 17 CpG sites, was significantly hypermethylated in all BC samples analyzed (Figure 18A). Importantly, about 87.5% of tumoral breast tissues evaluated (14 out of 16 BC samples) exhibit a significant hypermethylation in the whole CpG island analyzed with respect to the matched normal samples (Figure 18B), strongly indicating that the methylation in the CpG island of the *MPPED2* promoter is responsible for its reduction in BC. Furthermore, the *MPPED2* promoter methylation was even evaluated through bioinformatic analysis using the same TCGA BC cohort previously considered for its expression. Interestingly, *MPPED2* promoter was found significantly hypermethylated in 152 tumoral samples compared to 39 normal ones (Figure 18C), and a significant negative correlation was found between *MPPED2* expression and promoter methylation ($r=-0.4248$; $p<0.0001$) (Figure 18D), meaning that *MPPED2* reduction was more remarkable in CpG hypermethylated breast tumors. Taken together, these results strongly support that

the loss of *MPPED2* in cancer is mainly owing to the strong hypermethylation in the CpG islands of its promoter region.

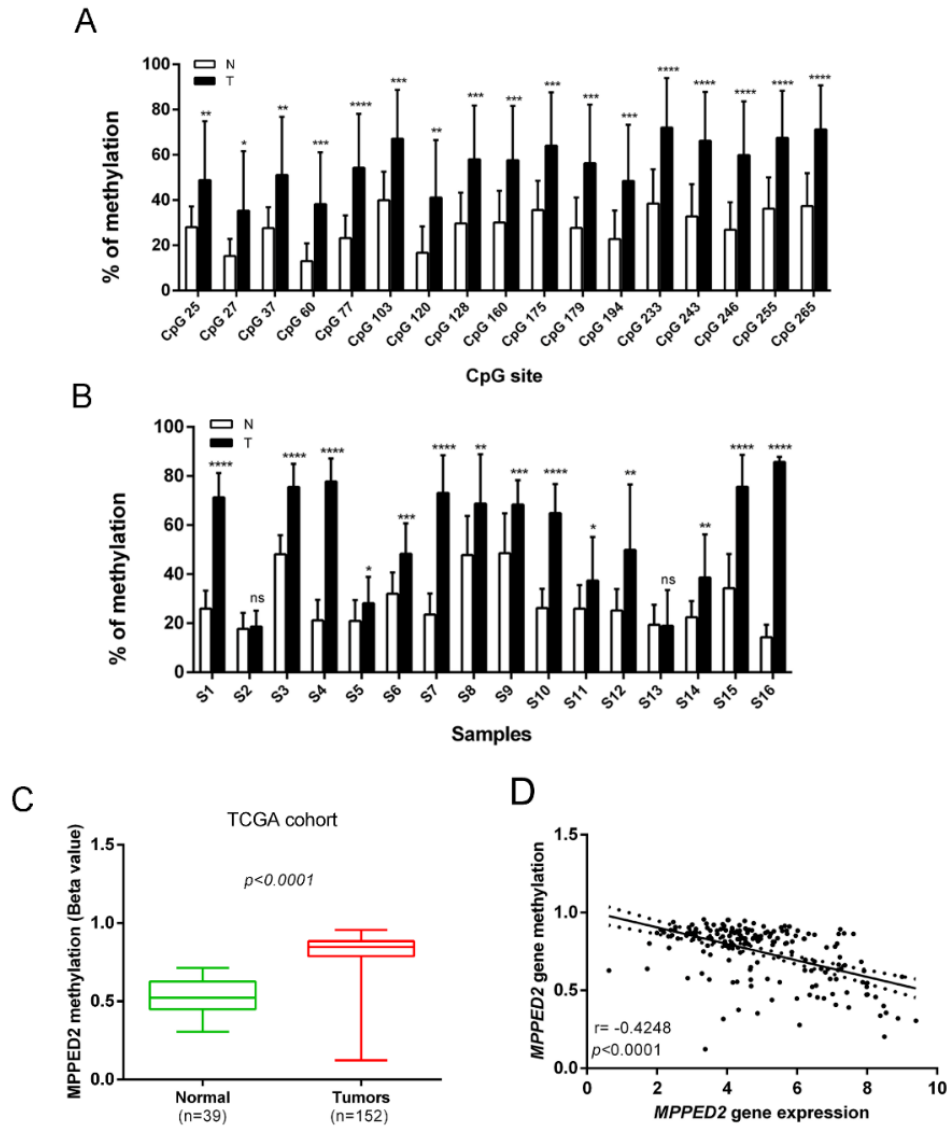


Figure 18. *MPPED2* methylation status in normal and tumoral samples. (A) Methylation levels of CpG sites in the *MPPED2* promoter. Each histogram represents the mean value of each CpG site in the whole cohort analyzed. White and black bars represent normal and breast cancer tissues, respectively. t-test: $p < 0.05$; $p < 0.01$; $p < 0.001$; $p < 0.0001$. (B) Methylation levels of the *MPPED2* promoter in each sample. Histograms represent the mean methylation value of all CpG sites in each sample. White and black bars represent normal and breast cancer tissues, respectively (S1-S16, different patient samples). t-test: $p < 0.05$; $p < 0.01$; $p < 0.001$; $p < 0.0001$; ns, not significant. (C) *MPPED2* methylation levels were evaluated in a dataset available at the TCGA comprising 152 breast tumors and 39 normal breast samples. t-test: $p < 0.0001$. (E) Correlation scatter plot

(Spearman's Rank) analysis between MPPED2 methylation values and expression levels in the TCGA cohort ($r = -0.4248$; $p < 0.0001$).

To validate that the reduction of MPPED2 in cancer is due to epigenetic regulation, MDA-MB-231, and SKBR3 BC cells, in which *MPPED2* expression was extremely low, were treated for 120 h with $2\mu\text{M}$ of the demethylating agent 5-Aza-2'-deoxycytidine (5-Aza-dC). After the treatment, MPPED2 levels were evaluated by qRT-PCR and Western blot analyses. Consistently, increased MPPED2 expression was obtained at both mRNA and protein levels in MDA-MB-231 and SKBR3 cells treated with 5-Aza-dC when compared with such cells treated with the DMSO vehicle (Figure 19A and 19B), confirming that *MPPED2* reduction in BC could be mainly due to the strong methylation of its regulatory regions.

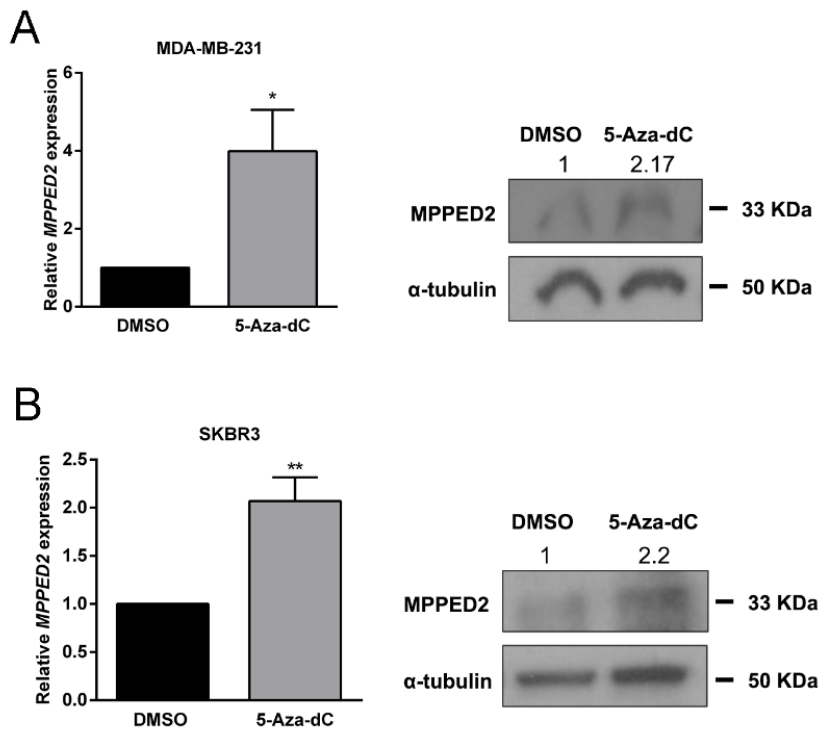


Figure 19. Analysis of MPPED2 expression levels after 5-Aza-dC treatment. (A, B) MPPED2 expression levels were evaluated by qRT-PCR in MDA-MB-231 and SKBR3 cell lines after $2\mu\text{M}$ 5-Aza-dC or DMSO (vehicle) treatment for 120 hours. Data were reported as mean \pm SD. t-test: $p < 0.05$; $p < 0.01$. MPPED2 protein expression was also evaluated by Western blot. Densitometric analysis of a representative experiment was performed by using ImageJ software. MPPED2 protein expression in 5-Aza-dC treatment was compared to vehicle (DMSO) treatment, set equal to 1.

4.5 The lncRNA *MPPED2-AS1* positive regulates *MPPED2* expression by binding *DNMT1*

Since *MPPED2* and *MPPED2-AS1* expression levels were significantly decreased and positively correlated in BC tissues, we aimed to investigate in detail their relationship in BC. To this aim, *MPPED2* expression levels were evaluated by qRT-PCR in MDA-MB-231 and SKBR3 cells in which the expression of *MPPED2-AS1* was restored. Intriguingly, a significant increase of *MPPED2* levels was detected in such cells (Figure 20A), strongly indicating that *MPPED2-AS1* is able to modulate *MPPED2* expression even in BC. Then, we observed an inverse correlation between *MPPED2-AS1* expression and *MPPED2* methylation (Figure 20B), leading us to suppose that this lncRNA might be able to modulate *MPPED2* expression through epigenetic regulation. Therefore, to deeper investigate whether an epigenetic modulation occurs, the methylation levels of *MPPED2* promoter were assessed in *MPPED2-AS1*-overexpressing BC cells by next-generation sequencing, after bisulfite treatment. As shown in Figure 20C, a significant reduction of *MPPED2* promoter methylation was detected in *MPPED2*-overexpressing cells in comparison with the EV, meaning that this lncRNA regulates *MPPED2* expression affecting the methylation pattern in its promoter region.

Consequently, to unveil the molecular mechanism by which *MPPED2-AS1* affects *MPPED2* methylation, we focus the attention on DNA methyltransferase enzyme 1 (DNMT1), an enzyme that catalyze the transfer of methyl group on DNA, since recent studies reported an innovative mechanism through which the lncRNAs are able to affect DNA methylation at locus-specific pattern by interacting with DNMT1 (Di Ruscio *et al.*, 2013, Merry *et al.*, 2015). Principally, DNMT1 is an enzyme known to play crucial role for maintenance methylation of several promoters of tumor suppressor genes (Bernardino *et al.*, 1997, Jair *et al.*, 2006, Lin *et al.*, 2007, Pathania *et al.*, 2015, Soares *et al.*, 1999). Therefore, we analyzed the expression levels of DNMT1 in the TCGA BC cohort used in this study. As reported in Figure 20D, high levels of *DNMT1* were found and a significant positive correlation between *MPPED2* methylation and *DNMT1* expression ($r=0.465$; $p<0.0001$) was observed (Figure 20E). Conversely, it is worth to note that a negative correlation between *DNMT1* and *MPPED2* expression was detected ($r=-0.4427$; $p<0.0001$) (Figure 20F), supporting the hypothesis regarding the involvement of DNMT1 in *MPPED2* promoter methylation.

Therefore, given this observation, to evaluate if *MPPED2-AS1* acts *via* DNMT1, we carried out the RNA immunoprecipitation (RIP) assay using a specific anti-DNMT1 antibody in SKBR3 cells. Accordingly, an enrichment of *MPPED2-AS1* in DNMT1 immunoprecipitated lysates was obtained when compared to the IgG controls (Figure 20G), confirming the interaction between DNMT1 and the lncRNA. Further, to evaluate if DNMT1 was effectively related to *MPPED2* promoter methylation, Chromatin immunoprecipitation (ChIP) assay was performed in SKBR3 cells transfected with *MPPED2-AS1*. To this aim, the crosslinked DNA-protein complexes were immunoprecipitated with a specific

antibody against DNMT1 or IgG. Immunoprecipitation of chromatin was then analyzed by qPCR examining a region spanning nucleotides -3500 related to the transcription start site (TSS) of the *MPPED2* promoter. As shown in Figure 20H, anti-DNMT1 antibodies precipitated *MPPED2* promoter in SKBR3 EV-transfected cell lines but not in those overexpressing *MPPED2-AS1*. Overall, these results indicate that *MPPED2-AS1* overexpression can increase *MPPED2* levels and in turn reduces DNA methylation at the *MPPED2* promoter region, likely through the binding with DNMT1.

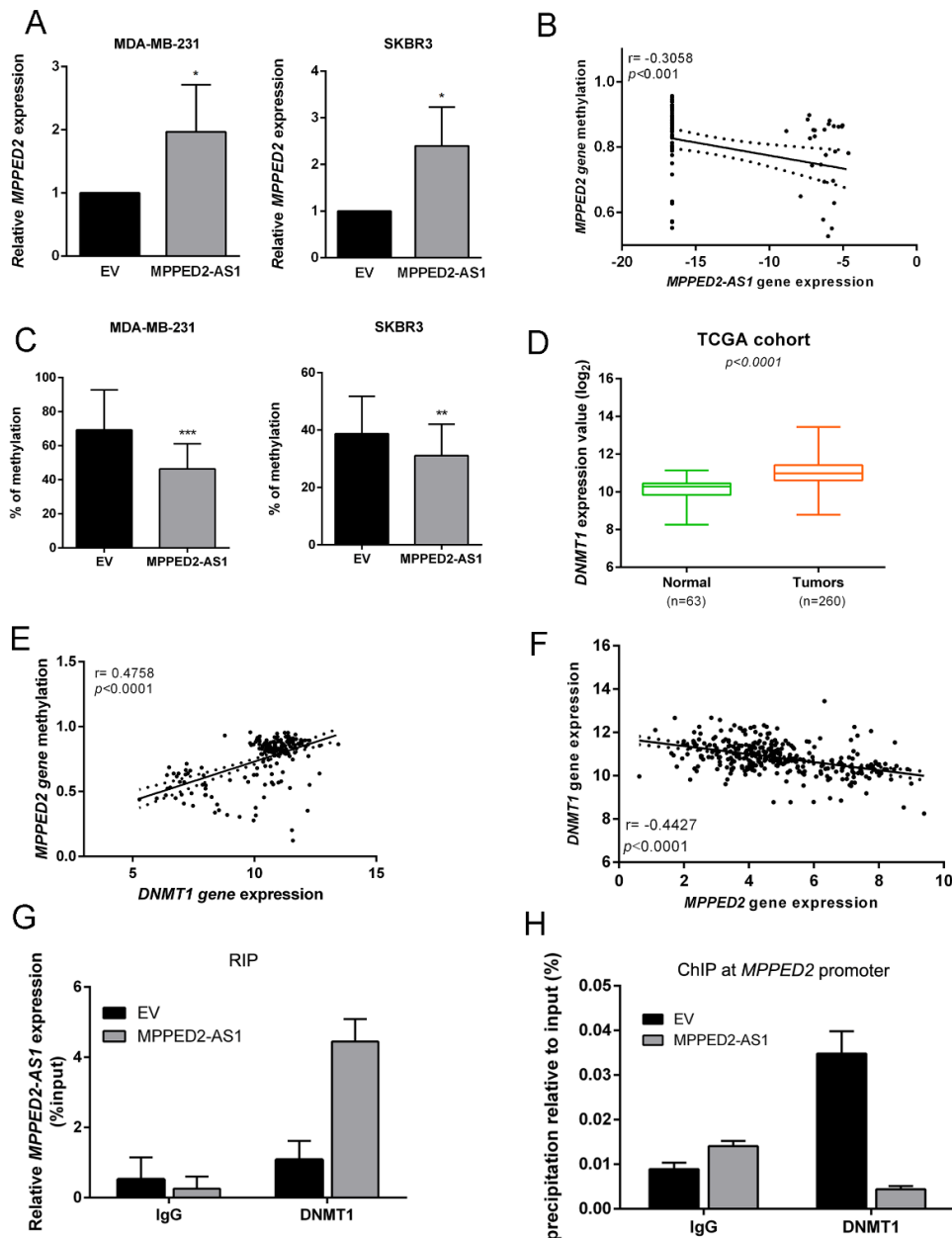


Figure 20. *MPPED2-AS1* interacts with DNMT1 decreasing *MPPED2* promoter methylation. (A) qRT-PCR analysis of *MPPED2* mRNA levels in BC cells transfected with *MPPED2-AS1*

overexpressing vector or the EV. Data are reported as $2^{-\Delta\Delta C_t}$ value \pm SD, compared to EV, set equal to 1. t-test: $p < 0.05$. (B) Correlation scatter plot (Spearman's Rank) between *MPPED2* methylation and *MPPED2-AS1* expression analyzed in the TCGA cohort ($r = -0.3058$; $p < 0.001$). (C) *MPPED2* promoter methylation levels were evaluated in BC cells transfected with *MPPED2-AS1* overexpressing vector or the EV. t-test: $p < 0.001$; $p < 0.01$. (D) *DNMT1* expression levels were evaluated in a dataset available in TCGA. $p < 0.0001$. (E) Correlation scatter plot (Spearman's Rank) between *DNMT1* expression and *MPPED2* methylation analyzed in the TCGA cohort ($r = 0.4756$; $p < 0.0001$). (F) Correlation scatter plot (Spearman's Rank) between *DNMT1* and *MPPED2* expression analyzed in the TCGA cohort ($r = -0.4427$; $p < 0.0001$). (G) RNA immunoprecipitation was performed on extracts obtained from SKBR3 cells transfected with *MPPED2-AS1* overexpressing vector or the EV, using an anti-DNMT1 antibody or a pre-immune (IgG) serum, as control. Immunoprecipitated *MPPED2-AS1* RNA was quantified by qRT-PCR. RNA levels were reported as percentage of input and were calculated with the $2^{-\Delta C_t}$ formula. (H) Chromatin immunoprecipitation (ChIP) assay was carried out in SKBR3 cells transiently transfected with *MPPED2* or the corresponding EV. SKBR3 cell lines were then crosslinked, sonicated and subjected to pre-clearing. The chromatin was immunoprecipitated using antibodies against DNMT1. IgG was used as negative control. The immunoprecipitated chromatin was analyzed by qPCR assay with primers specific for the *MPPED2* promoter.

4.6 *MPPED2* overexpression inhibits breast carcinoma cell growth

To better define the role of *MPPED2* in breast carcinogenesis we examined the effects of its overexpression on cellular proliferation and cell cycle regulation. To achieve this aim, first *MPPED2* expression was restored in MDA-MB-231 and SKBR3 cells by transfecting them with *MPPED2*-overexpressing vector. A great increase of *MPPED2* expression was detected in both BC cell systems by qRT-PCR and Western blot when compared with the BC cells transfected with the EV, confirming the stably ectopic *MPPED2* expression in both MDA-MB-231 and SKBR3 cells (Figure 21A and 21B).

Then, the proliferation rate of *MPPED2*-overexpressing BC cells was investigated. As shown in Figure 21C and 21D, MDA-MB-231-*MPPED2* and SKBR3-*MPPED2* were found to grow at a significantly slower rate in comparison with the EV control. Consistently, colony-formation assay was carried out in *MPPED2*-overexpressing BC cells, and the results demonstrated that *MPPED2* overexpression gave rise to a much lower number of colonies with respect to the EV (Fig. 21E and 21F), confirming that *MPPED2* slows down cell growth.

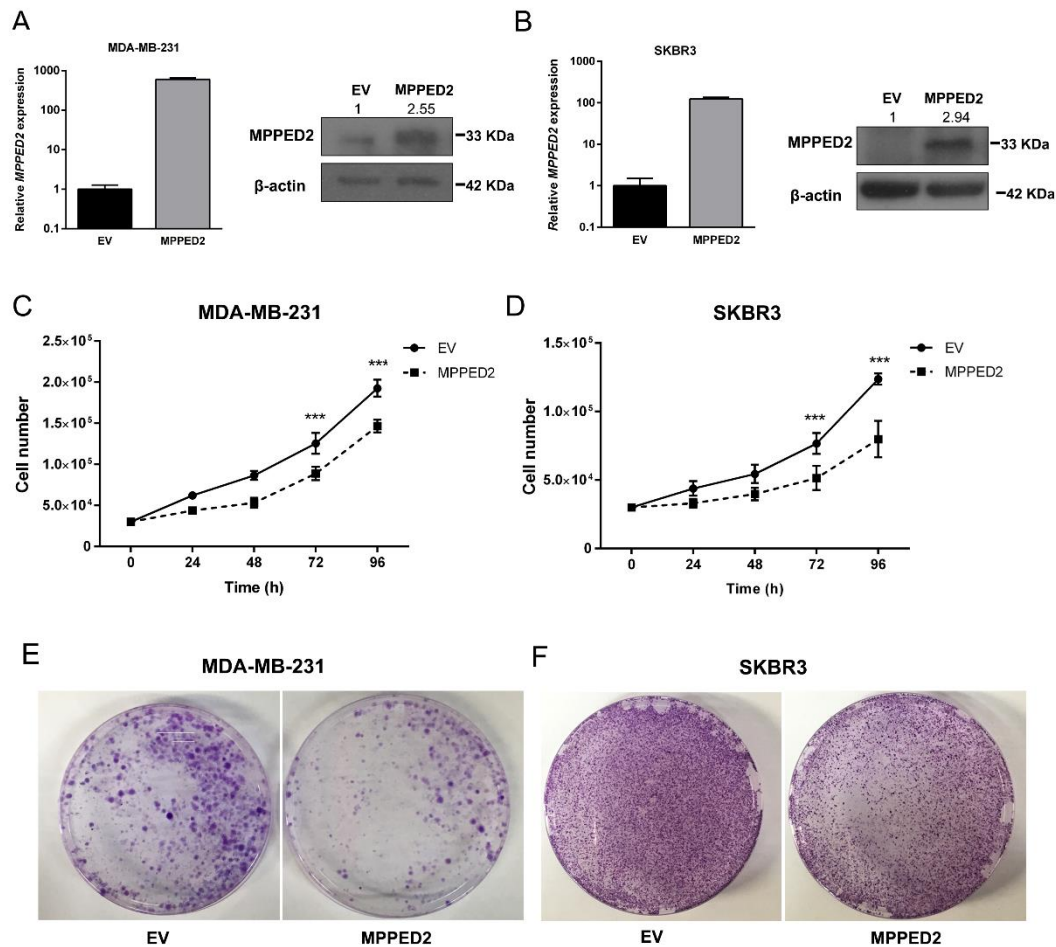


Figure 21. MPPED2 reduces cell proliferation of breast carcinoma cell lines. (A, B) qRT-PCR performed in BC cells stably expressing MPPED2 or carrying the corresponding EV. Data are reported as $2^{-\Delta\Delta C_t}$ values \pm SD, compared to the EV, set equal to 1. Western blot analysis confirming the expression of MPPED2. β -actin was used to normalize the amount of loaded protein. Densitometric analysis was performed by using ImageJ software to evaluate MPPED2 protein expression compared to EV, set equal to 1. (C, D) Cell growth analysis of BC cells stably expressing MPPED2 or carrying the corresponding EV. Cell number was evaluated at 24h, 48h, 72h, and 96h after seeding. Values were obtained from three independent experiments performed in duplicate. Data are reported as mean \pm SD. 2-way Anova test: $p < 0.001$. (E, F) Representative colony assays performed in BC cells transiently transfected with MPPED2 or the corresponding EV.

Subsequently, to study the effect of *MPPED2* overexpression on cell cycle progression, cell cycle distribution in *MPPED2*-overexpressing BC cells was evaluated by FACS analysis. Accordingly, a significant increase in G1 phase of MDA-MB-231-*MPPED2* (74.4% vs 54.15%; $p = 0.0286$, *MPPED2* vs control) and SKBR3-*MPPED2* (69.82% vs 51.88%; $p = 0.0079$, *MPPED2* vs control) cell number was detected in comparison with the control BC cells (Figure 22A and 22B). Furthermore, decreased cyclin D1 and cyclin E protein levels were found in both MDA-MB-231-*MPPED2* and SKBR3-*MPPED2* cells compared with the cells

transfected with the EV (Figure 22C). Taken together, these findings confirmed the negative regulation played by MPPED2 on BC cell proliferation through the downregulation of cyclin D1 and cyclin E and the accumulation of cells in the G1 phase of the cell cycle.

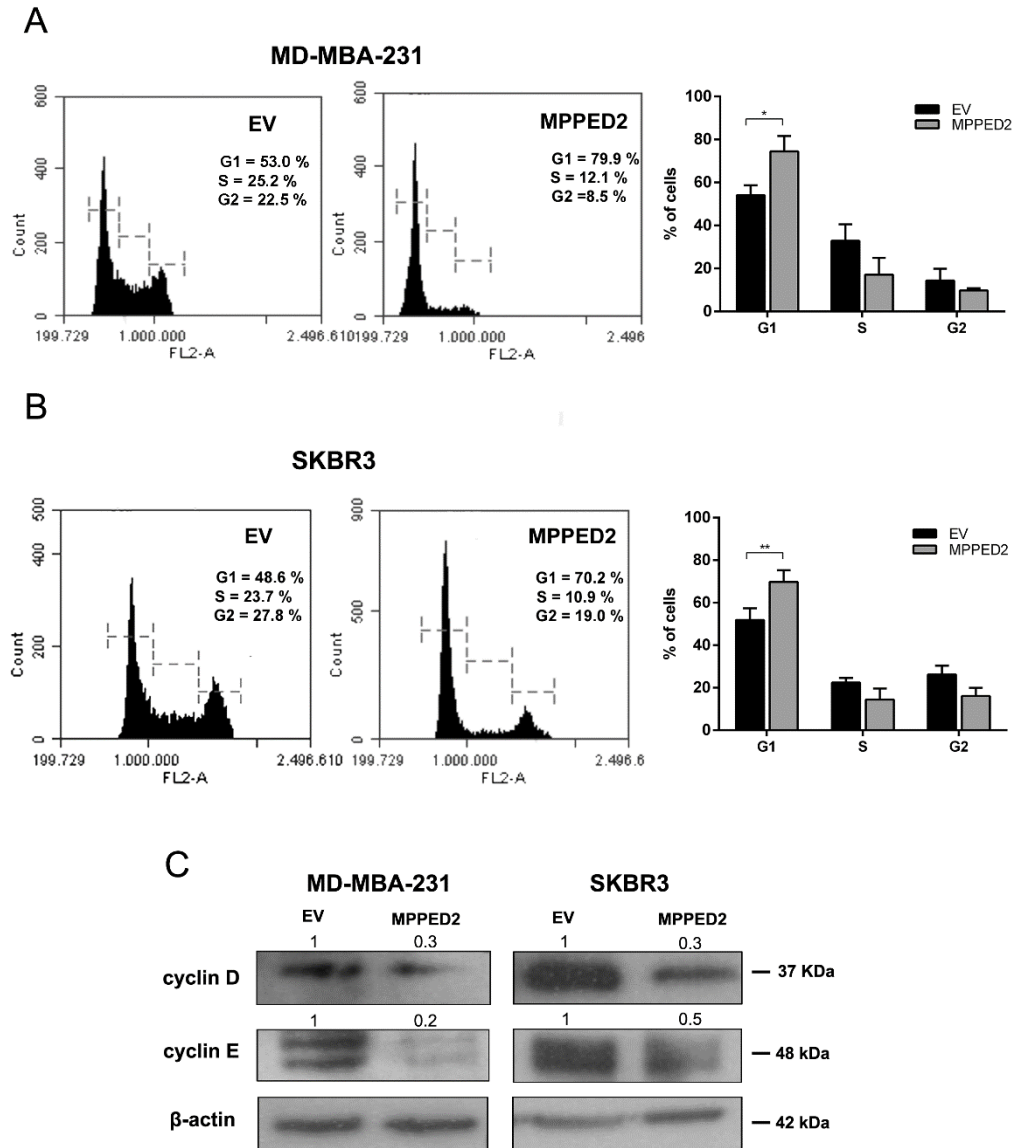


Figure 22. MPPED2 inhibits cell cycle progression of breast carcinoma cell lines. (A,B) Representative experiments of cell cycle analysis performed in MDA-MB-231 and SKBR3 cells stably transfected with MPPED2 or the corresponding EV are shown in the left panel. Values shown in the right panel were obtained from three independent experiments. t-test: $p=0.0286$; $p=0.0079$. (C) Western blot analysis of cyclin D and cyclin E expression in MD-MBA-231 and SKBR3 stably expressing MPPED2 or carrying the corresponding EV. β -actin was used to normalize the amount of loaded protein. Densitometric analysis was performed by using ImageJ software to analyze MPPED2 protein expression compared to the EV, set equal to 1.

4.7 Restoration of MPPED2 suppresses the malignant phenotype of BC cells

Next, to prove the involvement of *MPPED2* on breast cancer progression, we set up transwell and Matrigel invasion assays on MDA-MB-231-*MPPED2* and SKBR3-*MPPED2* stably transfected cells. The obtained data demonstrated that *MPPED2* overexpression is able to decrease cell migration and invasion ability of 40% ($p<0.01$) and 32% ($p<0.05$), respectively in MDA-MB-231 cells (Figure 23A). These data were also confirmed in SKBR3-*MPPED2* cells, where migration and invasion were reduced of about 60% ($p<0.05$) and 50% ($p<0.05$), respectively (Figure 23B).

Finally, the mechanism by which *MPPED2* affects migration and invasion was examined by evaluating ZEB1 and E-cadherin proteins through Western blot methodology. These genes are two important epithelial-mesenchymal transitions (EMT) markers (Eger *et al.*, 2005, Oka *et al.*, 1993, Schmalhofer *et al.*, 2009), thus, they are considered as hallmarks of tumor progression. Intriguingly, the reduction of ZEB1 and the increase of E-cadherin protein levels in *MPPED2*-overexpressing BC cells were observed (Figure 23C). Thereby, we can speculate that *MPPED2* modulates these two EMT markers and consequently it decreases BC cell migration and invasion *in vitro*. These results, further supporting the anti-oncogenic role of *MPPED2* in BC progression.

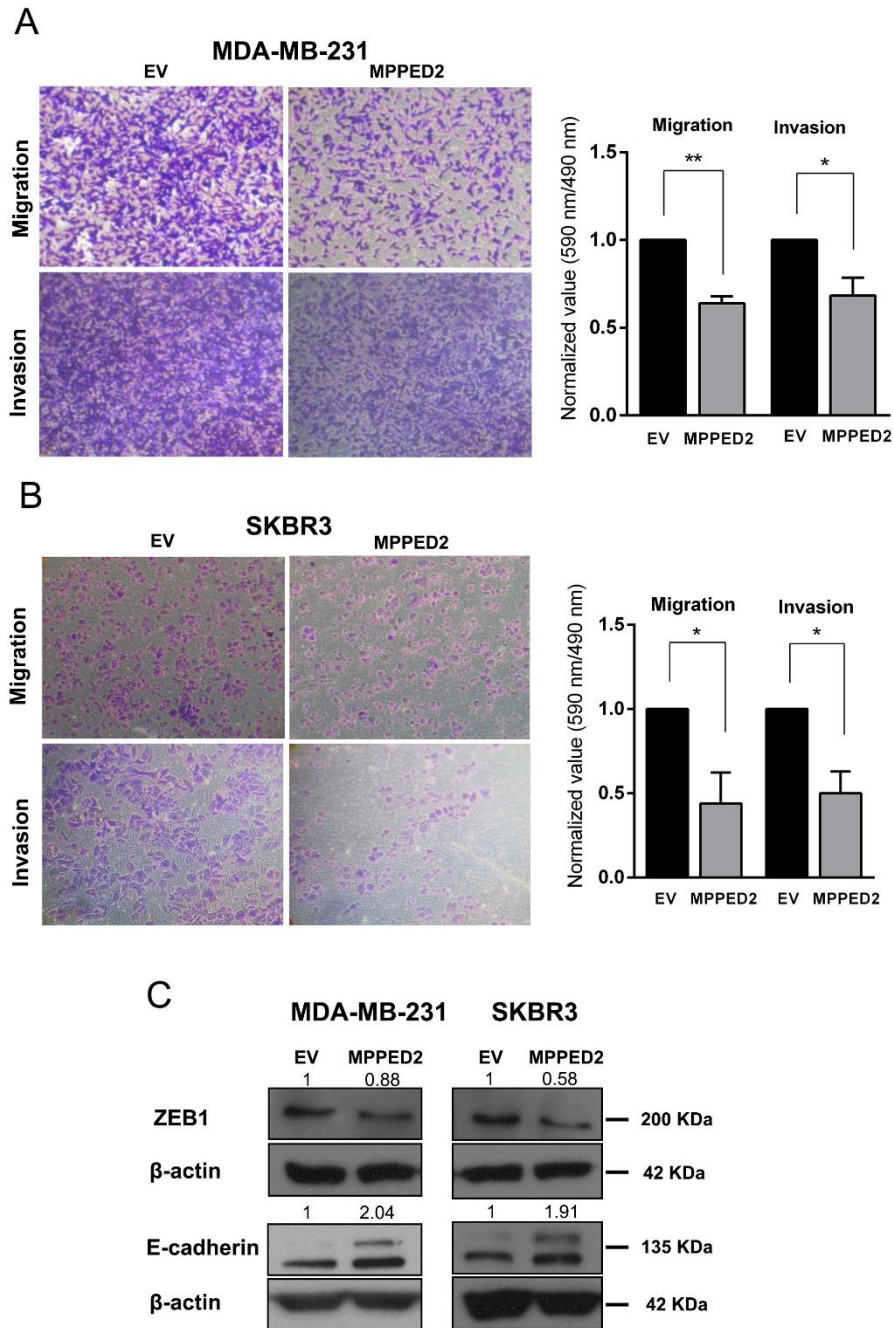


Figure 23. MPPED2 reduces cell migration and invasion of breast carcinoma cell lines. (A, B) Representative images of migration and invasion assays performed in BC cells stably transfected with MPPED2 or the corresponding EV (right panel). Magnification 40x. Data obtained from three independent experiments carried out in MDA-MB-231 and SKBR3 cells are shown in the left panel. Values are reported as mean value \pm SD, compared to the EV, set equal to 1. t-test: $p < 0.05$, $p < 0.01$. (C) Western blot analysis of ZEB1 and E-cadherin in MD-MBA-231 and SKBR3 cells stably expressing MPPED2 or carrying the corresponding EV. β -actin was used to normalize the amount of loaded protein. Densitometric analysis was performed by using ImageJ software to evaluate MPPED2 protein expression compared to EV, set equal to 1.

5. Discussion

In the present study, we have functional characterized the *MPPED2-AS1* and *MPPED2* roles in thyroid and breast carcinogenesis. First, through a human lncRNA microarray approach we identified a large number of DElncRNAs in twelve PTC compared to four normal thyroid tissues. After a stringent analysis based on p -value <0.001 and FDR <0.01 , we subsequently focused on the highly significant downregulated *MPPED2-AS1* lncRNA. Through bioinformatic analysis, we observed that *MPPED2-AS1* is located on chromosome 11 in an intronic antisense position with respect to *MPPED2*. This gene encodes a metallophosphodiesterase protein that belongs to III cyclic nucleotide metallophosphodiesterases family and located in a region whose deletion is associated with WAGR syndrome. Particularly, *MPPED2* showed opposite behaviour respect to the other cyclic PDE even though its functional role remains still unknown. Indeed, although several PDEs members have been found upregulated in cancers, data from literature demonstrated the potential tumor suppressor role of *MPPED2* in human cancer. Indeed, it has been recently demonstrated that the loss of *MPPED2* expression is an event that occurs in several malignant neoplasias originating from different tissues. Moreover, its restoration in cancer cell lines induces apoptosis and negatively modulates cell proliferation (Liguori *et al.*, 2012, Shen *et al.*, 2016, Zhang *et al.*, 2016), thus proposing *MPPED2* as a novel potential candidate tumor suppressor gene. Consequently, given the relevance of *MPPED2* in cancer and the significant reduction of the antisense lncRNA *MPPED2-AS1* in PTC, we decided to concentrate our study on the characterization of *MPPED2-AS1* and *MPPED2* in TC. Thus, we evaluated the expression of the *MPPED2-AS1* and *MPPED2* gene by qRT-PCR in a set of PTC samples and a strong reduction of these genes was observed respect to the non-tumoral thyroid tissues. Additionally, the expression analysis of both genes was extended in a set of TC histotypes of different malignancy, including benign FTA, the well differentiated PTC and FTC and the undifferentiated ATC samples. It is worth to note that the loss of such genes occurs gradually during TC progression, highlighting their involvement in TC. Importantly, a significant positive correlation was observed between *MPPED2* and *MPPED2-AS1* expression in the whole set of the analyzed thyroid neoplasm ($r=0.5604$; $p<0.001$), indicating that a co-regulation of these genes occurs in TC progression. Subsequently, functional studies were performed to define the role of *MPPED2-AS1* and *MPPED2* downregulation in thyroid carcinogenesis. Accordingly, we stably restored their expression in two TC cell system by using a vector expressing the lncRNA and/or the *MPPED2* sequences. We observed that both genes were able to reduce the cell proliferation and migration rate, thus indicating that the loss of *MPPED2-AS1* and *MPPED2* might contribute to the modulation of biological processes leading to TC development. Interestingly, we demonstrated the functional effects of *MPPED2-AS1* to induce the upregulation of the *MPPED2* gene expression in TC cells, indicating that the downregulated *MPPED2-AS1* and its associated-gene *MPPED2*,

could represent novel tumor suppressor genes with a considerable role in thyroid cell neoplastic transformation and progression.

The next step of this study was to evaluate whether the tumor suppressor roles of *MPPED2-AS1* and *MPPED2* described in thyroid neoplasia could be extended also to other human cancer types. Therefore, a preliminary bioinformatic analysis revealed that both genes were strongly downregulated in BC and, consequently, we investigated in detail their role also in this type of neoplasia. The results reported here demonstrate a significant downregulation of both genes in almost all human BC samples analyzed in comparison with the normal breast tissues, and a positive correlation between both genes was also detected in BC. Additionally, these findings were also supported through the evaluation of data available in the TCGA BC database. In fact, we observed a significant *MPPED2* and *MPPED2-AS1* reduction in many cases of BC as well as we also found that *MPPED2* expression levels were even lower in the main aggressive HER2 and TNBC subtypes, indicating that the *MPPED2* reduction might be correlated with the malignant BC phenotype. However, IHC analysis performed on BC TMA confirmed the decreased *MPPED2* levels in BC tissues even though no correlation was observed with *MPPED2* expression and the clinicopathological features of BC patients. This excludes the possibility to use *MPPED2* as a prognostic marker but its detection through qRT-PCR and IHC might represent a new tool for the diagnosis of breast neoplasia.

DNA methylation is a key epigenetic hallmark typically associated with the silencing of anti-tumoral genes in mammalian cells (Wu and Zhang 2014). Whole-genome approaches have lately been used to explain breast-cancer-specific DNA methylation signatures so far. In fact, it becomes clear that the silencing of tumor suppressor genes by DNA methylation provides an important molecular mechanism by which this epigenetic alteration can trigger cancer, and provides a new therapeutic strategy aimed at inhibition of DNA methylation and re-expression of repressed tumor suppressor genes (Hansen *et al.*, 2011). Given that DNA methylation changes are critical factors involved in BC, we have examined the plausible mechanism responsible for *MPPED2* reduction in cancer by analyzing the methylation of its promoter in human BC tissues through bisulfite sequencing. By this approach, a strong methylation of *MPPED2* promoter was detected in 14 out of 16 BC (87.5%) samples analyzed with respect to the normal ones. Surprisingly, all 17 CpG sites within the *MPPED2* promoter region were significantly hypermethylated when compared to each normal breast tissue. Moreover, our findings were also confirmed through the evaluation of methylation data available in the TCGA BC database, confirming that *MPPED2* promoter was significantly hypermethylated in breast primary tumors respect to the normal breast tissues. Importantly, a negative correlation between *MPPED2* promoter methylation and its gene expression was observed in the TCGA BC dataset, indicating that the suppression of *MPPED2* expression was more pronounced in tumors with CpG hypermethylation. Consistently, the treatment with the demethylating agent 5-Aza-dC induces re-expression of *MPPED2* in BC cell systems at both transcriptional

and translational levels, supporting the idea that *MPPED2* hypermethylation accounts for its downregulation in BC. Interestingly, the *MPPED2* promoter was more recently found hypermethylated also in colorectal cancer (CRC) (Gu *et al.*, 2019). Indeed, it has been observed a significant positive correlation between *MPPED2* promoter methylation and the malignant phenotype of CRC, thus this finding lead to consider *MPPED2* as a powerful marker for risk assessment in CRC, and further supporting that DNA methylation in the *MPPED2* promoter region might be the main mechanism responsible for its reduction in cancer.

Recently, many studies have revealed that lncRNAs are involved in the aberrant DNA methylation pattern during carcinogenesis. In fact, accumulating evidence implies that lncRNAs could interact with DNA methyltransferase enzymes (main regulators of DNA methylation in mammals) and, consequently, affect their genomic occupancy or activity (Di Ruscio *et al.*, 2013, Merry *et al.*, 2015, Qi *et al.*, 2016). Given this consideration, we investigated whether our lncRNA *MPPED2-AS1* is implicated in this epigenetic modification since we observed that the lncRNA can positively regulate *MPPED2* expression in MDA-MB-231 and SKBR3 cell lines. Interestingly, we found that *MPPED2-AS1* overexpression was able to reduce the *MPPED2* promoter methylation in BC cells, and, interestingly, a significant inverse correlation between *MPPED2* methylation and *MPPED2-AS1* expression was observed in the BC TCGA cohort. As far as epigenetic regulations are concerned, we supposed that the lncRNA can modulate *MPPED2* expression by affecting its methylation status. Therefore, with the evidence in literature that many lncRNAs are able to modulate global gene expression through the interaction with DNMT1, we investigated this mechanism. Therefore, first through the evaluation of data of the TCGA database, we observed either an increased expression of *DNMT1* in BC samples as well as a positive correlation between *DNMT1* expression and *MPPED2* methylation. Conversely, a negative one between *DNMT1* and *MPPED2* expression in the BC TCGA dataset was found, indicating that DNMT1 upregulation may participate to *MPPED2* promoter hypermethylation. Additionally, we demonstrated that *MPPED2-AS1* directly interacts with DNMT1 and, intriguingly, that the binding of DNMT1 at *MPPED2* promoter was decreased in SKBR3-*MPPED2-AS1* cells. Overall, our finding indicated that *MPPED2-AS1* positively modulates *MPPED2* expression through the binding with DNMT1, thus preventing DNMT1-mediated methylation of *MPPED2* CpG islands in the promoter region in BC. However, we cannot exclude that other epigenetic regulations might be involved in the modulation of the *MPPED2* gene expression.

Subsequently, functional studies were carried out to evaluate the role of *MPPED2* in breast carcinogenesis, after its restoration in MDA-MB-231 and SKBR3, in which *MPPED2* expression is very low. Consistently, the cell growth assays reported that *MPPED2* overexpression was able to inhibit cell proliferation and induced a delay in the transition from G0/G1 to the S phase of BC cell lines. Additionally, a strong reduction of cyclin D and cyclin E protein levels was also detected by Western blot analysis, suggesting a crucial role of *MPPED2* in the

control of this phase of cell cycle. Moreover, we found that *MPPED2* overexpression was able to inhibit cell migration and invasion, supporting the anti-oncogenic role of *MPPED2* and, thereby, the contribution of its downregulation to BC development. Furthermore, we observed that *MPPED2* restoration was able to reduce ZEB1 and to increase E-cadherin protein levels, two key proteins involved in EMT, thus suggesting that *MPPED2* could exert its tumor suppressor activity by modulating this signaling pathway (Eger *et al.*, 2005, Oka *et al.*, 1993, Schmalhofer *et al.*, 2009). However, further studies are required to investigate the mechanism by which *MPPED2* exerts its anti-oncogenic role. According to the literature, *MPPED2* is downregulated in some human cancer, including neuroblastoma (Liguori *et al.*, 2012), cervical cancer (Zhang *et al.*, 2016) and oral squamous carcinoma (Shen *et al.*, 2016), indicating that its anti-oncogenic role is not confined to few neoplastic histotypes. Moreover, preliminary results obtained by our research group have detected *MPPED2* reduction also in glioblastoma multiforme (GBM). More in deep, using data available from TCGA, Gravendeel and Remembrant databases it appears evident that among the different GBM subtype (Proneural, Neural, Classical and Mesenchymal), *MPPED2* showed the lowest expression in the main aggressive Mesenchymal one, suggesting once more its critical role during carcinogenesis. Furthermore, we are going to perform further study to better characterize the *MPPED2* role in GBM and to assess whether *MPPED2* could be able to reduce the resistance of GBM to Temozolomide drug, verifying whether its expression may be important for the regulation of sensitivity to chemotherapy drug. However, we could exclude *MPPED2* downregulation as a feature of all human malignancies, since some human cancers as liver, lung and prostate carcinomas did not display any reduction of *MPPED2* expression, as evaluated on TCGA dataset. Overall, these results indicate the functional significance of *MPPED2* overexpression as it relates to cell cycle inhibition, reduction of migration and invasion, representing unique opposite functions to other known PDE classes I and II.

6. Conclusion

In this study, we identified several lncRNAs whose expression is deregulated in PTC compared to normal thyroid samples and, among them, we focused on *MPPED2-AS1* and its associated-antisense gene *MPPED2* for further investigations. We report that both genes are downregulated in thyroid neoplasia. Moreover, the restoration of their expression in TC cell lines reduces cell proliferation and migration, thus suggesting a tumor suppressor role for *MPPED2-AS1* and *MPPED2* in the development of thyroid neoplasia.

Additionally, our findings demonstrate the tumor suppressor roles of *MPPED2-AS1* and *MPPED2* also in BC. In particular, we reported that *MPPED2* and *MPPED2-AS1* are significantly downregulated in BC tissues and cells. It also confirmed that the hypermethylation of *MPPED2* promoter accounted for its downregulation in BC, and importantly, its antisense lncRNA *MPPED2-AS1* positively regulated *MPPED2* likely through epigenetic regulation. In fact, the reduction of *MPPED2-AS1* led to the increasing hypermethylation of *MPPED2* promoter in BC. Interestingly, we found that *MPPED2-AS1* physically binds DNMT1, which could be responsible for *MPPED2* promoter methylation in breast cancer. Furthermore, the study demonstrates that restoration of *MPPED2* expression causes a delay of cell growth and inhibits cell migration and invasion of BC cells, suggesting that re-expression of *MPPED2* may be important for therapeutic use to impair cancer progression.

7. List of publications

1. **Pellecchia S**, Sepe R, Decaussin-Petrucci M, Ivan C, Masayoshi S, Coppola C, Testa D, Calin GA, Fusco A, Pallante P. The long non-coding RNA Prader Willi/Angelman region RNA5 (PAR5) is downregulated in anaplastic thyroid carcinomas where it acts as a tumor suppressor by reducing EZH2 expression and activity. *Cancers (Basel)*. 2020 Jan 17;12(1). pii: E235. doi: 10.3390/cancers12010235.
2. **Pellecchia S**, Sepe R, Federico A, Cuomo M, Credendino SC, Pisapia P, Bellevicine C, Nicolau-Neto P, Severo Ramundo M, Crescenzi E, De Vita G, Terracciano LM, Chiariotti L, Fusco A, Pallante P. The Metallophosphoesterase-Domain-Containing Protein 2 (MPPED2) Gene Acts as Tumor Suppressor in Breast Cancer. *Cancers (Basel)*. 2019 Jun 8;11(6). pii: E797. doi: 10.3390/cancers11060797.
3. D'Angelo D, Mussnich P, Sepe R, Raia M, Del Vecchio L, Cappabianca P, **Pellecchia S**, Petrosino S, Saggio S, Solari D, Fraggetta F, Fusco A. RPSAP52 lncRNA is overexpressed in pituitary tumors and promotes cell proliferation by acting as miRNA sponge for HMGA proteins. *J Mol Med (Berl)*. 2019 Jul;97(7) 1019-1032. doi: 10.1007/s00109-019-01789-7.
4. **Pellecchia S**, Quintavalle C, Pallante P. The control of tumor progression by circular RNAs: Novel prognostic and therapeutic insights resulting from the analysis of the circAGO2/human antigen R complex. *Translational Cancer Research*. doi: 10.21037/tcr.2019.03.10
5. Capo A, Sepe R, Pellino G, Milone M, Malapelle U, **Pellecchia S**, Pepe F, Cacciola NA, Manigrasso M, Bruzzaniti S, Sciaudone G, De Palma GD, Galgani M, Selvaggi F, Troncone G, Fusco A, D'Auria S, Pallante P. Setting up and exploitation of a nano/technological platform for the evaluation of HMGA1b protein in peripheral blood of cancer patients. *Nanomedicine*. 2019 Jan;15(1):231-242. doi: 10.1016/j.nano.2018.09.011. Epub 2018 Oct 9.
6. Sepe R, **Pellecchia S**, Serra P, D'Angelo D, Federico A, Raia M, Cortez Cardoso Penha R, Decaussin-Petrucci M, Del Vecchio L, Fusco A, Pallante P. The Long Non-Coding RNA RP5-1024C24.1 and Its Associated-Gene MPPED2 Are Down-Regulated in Human Thyroid Neoplasias and Act as Tumour Suppressors. *Cancers (Basel)*. 2018 May 18;10(5). pii: E146. doi: 10.3390/cancers10050146.
7. Penha RCC, **Pellecchia S**, Pacelli R, Pinto LFR, Fusco A. Ionizing Radiation Deregulates the MicroRNA Expression Profile in Differentiated Thyroid Cells. *Thyroid*. 2018 Mar;28(3):407-421. doi: 10.1089/thy.2017.0458.

8. Penha RCC, Sepe R, De Martino M, Esposito F, **Pellecchia S**, Raia M, Del Vecchio L, Decaussin-Petrucci M, De Vita G, Pinto LFR, Fusco A. Role of Dicer1 in thyroid cell proliferation and differentiation. *Cell Cycle*. 2017;16(23):2282-2289. doi: 10.1080/15384101.2017.1380127. Epub 2017 Nov 9.
9. Forzati F, De Martino M, Esposito F, Sepe R, **Pellecchia S**, Malapelle U, Pellino G, Arra C, Fusco A. miR-155 is positively regulated by CBX7 in mouse embryonic fibroblasts and colon carcinomas, and targets the KRAS oncogene. *BMC Cancer*. 2017 Mar 4;17(1):170. doi: 10.1186/s12885-017-3158-z.
10. De Martino M, Forzati F, Marfella M, **Pellecchia S**, Arra C, Terracciano L, Fusco A, Esposito F. HMGA1P7-pseudogene regulates H19 and Igf2 expression by a competitive endogenous RNA mechanism. *Sci Rep*. 2016 Nov 22;6:37622. doi: 10.1038/srep37622.
11. Palumbo A Jr, Da Costa NM, De Martino M, Sepe R, **Pellecchia S**, de Sousa VP, Nicolau Neto P, Krueel CD, Bergman A, Nasciutti LE, Fusco A, Pinto LF. UBE2C is overexpressed in ESCC tissues and its abrogation attenuates the malignant phenotype of ESCC cell lines. *Oncotarget*. 2016 Oct 4;7(40):65876-65887. doi: 10.18632/oncotarget.11674.
12. Cacciola NA, Sepe R, Forzati F, Federico A, **Pellecchia S**, Malapelle U, De Stefano A, Rocco D, Fusco A, Pallante P. Restoration of CBX7 expression increases the susceptibility of human lung carcinoma cells to irinotecan treatment. *Naunyn-Schmiedeberg's Arch Pharmacol*. 2015 Nov;388(11):1179-86. doi: 10.1007/s00210-015-1153-y. Epub 2015 Jul 28.

8. References

1. Crick FH. On protein synthesis. *Symp Soc Exp Biol* **1958**;12:138-63
2. Ponting CP, Oliver PL, Reik W. Evolution and functions of long noncoding RNAs. *Cell* **2009**;136:629-41
3. Mercer TR, Dinger ME, Mattick JS. Long non-coding RNAs: insights into functions. *Nat Rev Genet* **2009**;10:155-9
4. Amaral PP, Dinger ME, Mercer TR, Mattick JS. The eukaryotic genome as an RNA machine. *Science* **2008**;319:1787-9
5. Collins LJ, Chen XS. Ancestral RNA: the RNA biology of the eukaryotic ancestor. *RNA Biol* **2009**;6:495-502
6. Collins LJ, Penny D. The RNA infrastructure: dark matter of the eukaryotic cell? *Trends Genet* **2009**;25:120-8
7. Mattick JS. The genetic signatures of noncoding RNAs. *PLoS Genet* **2009**;5:e1000459
8. He L, Hannon GJ. MicroRNAs: small RNAs with a big role in gene regulation. *Nat Rev Genet* **2004**;5:522-31
9. Mendell JT. MicroRNAs: critical regulators of development, cellular physiology and malignancy. *Cell Cycle* **2005**;4:1179-84
10. Croce CM. Causes and consequences of microRNA dysregulation in cancer. *Nat Rev Genet* **2009**;10:704-14
11. Esquela-Kerscher A, Slack FJ. Oncomirs - microRNAs with a role in cancer. *Nat Rev Cancer* **2006**;6:259-69
12. Hammond SM. MicroRNAs as tumor suppressors. *Nat Genet* **2007**;39:582-3
13. Nicoloso MS, Spizzo R, Shimizu M, Rossi S, Calin GA. MicroRNAs--the micro steering wheel of tumour metastases. *Nat Rev Cancer* **2009**;9:293-302
14. Carninci P, Kasukawa T, Katayama S, Gough J, Frith MC, Maeda N, Oyama R, Ravasi T, Lenhard B, Wells C, Kodzius R, Shimokawa K, Bajic VB, Brenner SE, Batalov S, Forrest AR, Zavolan M, Davis MJ, Wilming LG, Aidinis V, Allen JE, Ambesi-Impiombato A, Apweiler R, Aturaliya RN, Bailey TL, Bansal M, Baxter L, Beisel KW, Bersano T, Bono H, Chalk AM, Chiu KP, Choudhary V, Christoffels A, Clutterbuck DR, Crowe ML, Dalla E, Dalrymple BP, de Bono B, Della Gatta G, di Bernardo D, Down T, Engstrom P, Fagiolini M, Faulkner G, Fletcher CF, Fukushima T, Furuno M, Futaki S, Gariboldi M, Georgii-Hemming P, Gingeras TR, Gojobori T, Green RE, Gustincich S, Harbers M, Hayashi Y, Hensch TK, Hirokawa N, Hill D, Huminiecki L, Iacono M, Ikeo K, Iwama A, Ishikawa T, Jakt M, Kanapin A, Katoh M, Kawasawa Y, Kelso J, Kitamura H, Kitano H, Kollias G, Krishnan SP, Kruger A, Kummerfeld SK, Kurochkin IV, Lareau LF, Lazarevic D, Lipovich L, Liu J, Liuni S, McWilliam S, Madan Babu M, Madera M, Marchionni L, Matsuda H, Matsuzawa S, Miki H, Mignone F, Miyake S, Morris K, Mottagui-Tabar S, Mulder N, Nakano N, Nakauchi H, Ng P, Nilsson R, Nishiguchi S, Nishikawa S, Nori F, Ohara O, Okazaki Y, Orlando V, Pang KC, Pavan WJ,

- Pavesi G, Pesole G, Petrovsky N, Piazza S, Reed J, Reid JF, Ring BZ, Ringwald M, Rost B, Ruan Y, Salzberg SL, Sandelin A, Schneider C, Schonbach C, Sekiguchi K, Semple CA, Seno S, Sessa L, Sheng Y, Shibata Y, Shimada H, Shimada K, Silva D, Sinclair B, Sperling S, Stupka E, Sugiura K, Sultana R, Takenaka Y, Taki K, Tammoja K, Tan SL, Tang S, Taylor MS, Tegner J, Teichmann SA, Ueda HR, van Nimwegen E, Verardo R, Wei CL, Yagi K, Yamanishi H, Zabarovsky E, Zhu S, Zimmer A, Hide W, Bult C, Grimmond SM, Teasdale RD, Liu ET, Brusic V, Quackenbush J, Wahlestedt C, Mattick JS, Hume DA, Kai C, Sasaki D, Tomaru Y, Fukuda S, Kanamori-Katayama M, Suzuki M, Aoki J, Arakawa T, Iida J, Imamura K, Itoh M, Kato T, Kawaji H, Kawagashira N, Kawashima T, Kojima M, Kondo S, Konno H, Nakano K, Ninomiya N, Nishio T, Okada M, Plessy C, Shibata K, Shiraki T, Suzuki S, Tagami M, Waki K, Watahiki A, Okamura-Oho Y, Suzuki H, Kawai J, Hayashizaki Y, Consortium F, Group RGER, Genome Science G. The transcriptional landscape of the mammalian genome. *Science* **2005**;309:1559-63
15. Kapranov P, Cheng J, Dike S, Nix DA, Duttagupta R, Willingham AT, Stadler PF, Hertel J, Hackermuller J, Hofacker IL, Bell I, Cheung E, Drenkow J, Dumais E, Patel S, Helt G, Ganesh M, Ghosh S, Piccolboni A, Sementchenko V, Tammana H, Gingeras TR. RNA maps reveal new RNA classes and a possible function for pervasive transcription. *Science* **2007**;316:1484-8
16. Wang KC, Yang YW, Liu B, Sanyal A, Corces-Zimmerman R, Chen Y, Lajoie BR, Protacio A, Flynn RA, Gupta RA, Wysocka J, Lei M, Dekker J, Helms JA, Chang HY. A long noncoding RNA maintains active chromatin to coordinate homeotic gene expression. *Nature* **2011**;472:120-4
17. Guttman M, Amit I, Garber M, French C, Lin MF, Feldser D, Huarte M, Zuk O, Carey BW, Cassady JP, Cabili MN, Jaenisch R, Mikkelsen TS, Jacks T, Hacohen N, Bernstein BE, Kellis M, Regev A, Rinn JL, Lander ES. Chromatin signature reveals over a thousand highly conserved large non-coding RNAs in mammals. *Nature* **2009**;458:223-7
18. Cabili MN, Trapnell C, Goff L, Koziol M, Tazon-Vega B, Regev A, Rinn JL. Integrative annotation of human large intergenic noncoding RNAs reveals global properties and specific subclasses. *Genes Dev* **2011**;25:1915-27
19. Derrien T, Johnson R, Bussotti G, Tanzer A, Djebali S, Tilgner H, Guernec G, Martin D, Merkel A, Knowles DG, Lagarde J, Veeravalli L, Ruan X, Ruan Y, Lassmann T, Carninci P, Brown JB, Lipovich L, Gonzalez JM, Thomas M, Davis CA, Shiekhhattar R, Gingeras TR, Hubbard TJ, Notredame C, Harrow J, Guigo R. The GENCODE v7 catalog of human long noncoding RNAs: analysis of their gene structure, evolution, and expression. *Genome Res* **2012**;22:1775-89
20. Cabili MN, Dunagin MC, McClanahan PD, Biaesch A, Padovan-Merhar O, Regev A, Rinn JL, Raj A. Localization and abundance analysis of human lncRNAs at single-cell and single-molecule resolution. *Genome Biol* **2015**;16:20
21. Rackham O, Shearwood AM, Mercer TR, Davies SM, Mattick JS, Filipovska A. Long noncoding RNAs are generated from the mitochondrial genome and regulated by nuclear-encoded proteins. *RNA* **2011**;17:2085-93

22. Rinn JL, Chang HY. Genome regulation by long noncoding RNAs. *Annu Rev Biochem* **2012**;81:145-66
23. Yan B, Wang Z. Long noncoding RNA: its physiological and pathological roles. *DNA Cell Biol* **2012**;31 Suppl 1:S34-41
24. Khalil AM, Guttman M, Huarte M, Garber M, Raj A, Rivea Morales D, Thomas K, Presser A, Bernstein BE, van Oudenaarden A, Regev A, Lander ES, Rinn JL. Many human large intergenic noncoding RNAs associate with chromatin-modifying complexes and affect gene expression. *Proc Natl Acad Sci U S A* **2009**;106:11667-72
25. Long Y, Wang X, Youmans DT, Cech TR. How do lncRNAs regulate transcription? *Sci Adv* **2017**;3:eaa02110
26. Guttman M, Donaghey J, Carey BW, Garber M, Grenier JK, Munson G, Young G, Lucas AB, Ach R, Bruhn L, Yang X, Amit I, Meissner A, Regev A, Rinn JL, Root DE, Lander ES. lincRNAs act in the circuitry controlling pluripotency and differentiation. *Nature* **2011**;477:295-300
27. Ciaudo C, Bourdet A, Cohen-Tannoudji M, Dietz HC, Rougeulle C, Avner P. Nuclear mRNA degradation pathway(s) are implicated in Xist regulation and X chromosome inactivation. *PLoS Genet* **2006**;2:e94
28. Tsai MC, Manor O, Wan Y, Mosammamparast N, Wang JK, Lan F, Shi Y, Segal E, Chang HY. Long noncoding RNA as modular scaffold of histone modification complexes. *Science* **2010**;329:689-93
29. Gupta RA, Shah N, Wang KC, Kim J, Horlings HM, Wong DJ, Tsai MC, Hung T, Argani P, Rinn JL, Wang Y, Brzoska P, Kong B, Li R, West RB, van de Vijver MJ, Sukumar S, Chang HY. Long non-coding RNA HOTAIR reprograms chromatin state to promote cancer metastasis. *Nature* **2010**;464:1071-6
30. Batista PJ, Chang HY. Long noncoding RNAs: cellular address codes in development and disease. *Cell* **2013**;152:1298-307
31. Fatica A, Bozzoni I. Long non-coding RNAs: new players in cell differentiation and development. *Nat Rev Genet* **2014**;15:7-21
32. Mercer TR, Mattick JS. Structure and function of long noncoding RNAs in epigenetic regulation. *Nat Struct Mol Biol* **2013**;20:300-7
33. Yoon JH, Abdelmohsen K, Srikantan S, Yang X, Martindale JL, De S, Huarte M, Zhan M, Becker KG, Gorospe M. LincRNA-p21 suppresses target mRNA translation. *Mol Cell* **2012**;47:648-55
34. Tripathi V, Ellis JD, Shen Z, Song DY, Pan Q, Watt AT, Freier SM, Bennett CF, Sharma A, Bubulya PA, Blencowe BJ, Prasanth SG, Prasanth KV. The nuclear-retained noncoding RNA MALAT1 regulates alternative splicing by modulating SR splicing factor phosphorylation. *Mol Cell* **2010**;39:925-38
35. Gong C, Maquat LE. lncRNAs transactivate STAU1-mediated mRNA decay by duplexing with 3' UTRs via Alu elements. *Nature* **2011**;470:284-8
36. Cheetham SW, Gruhl F, Mattick JS, Dinger ME. Long noncoding RNAs and the genetics of cancer. *Br J Cancer* **2013**;108:2419-25
37. Gibb EA, Brown CJ, Lam WL. The functional role of long non-coding RNA in human carcinomas. *Mol Cancer* **2011**;10:38

38. Hauptman N, Glavac D. Long non-coding RNA in cancer. *Int J Mol Sci* **2013**;14:4655-69
39. Mitra SA, Mitra AP, Triche TJ. A central role for long non-coding RNA in cancer. *Front Genet* **2012**;3:17
40. Zhang H, Chen Z, Wang X, Huang Z, He Z, Chen Y. Long non-coding RNA: a new player in cancer. *J Hematol Oncol* **2013**;6:37
41. Calin GA, Liu CG, Ferracin M, Hyslop T, Spizzo R, Sevignani C, Fabbri M, Cimmino A, Lee EJ, Wojcik SE, Shimizu M, Tili E, Rossi S, Taccioli C, Pichiorri F, Liu X, Zupo S, Herlea V, Gramantieri L, Lanza G, Alder H, Rassenti L, Volinia S, Schmittgen TD, Kipps TJ, Negrini M, Croce CM. Ultraconserved regions encoding ncRNAs are altered in human leukemias and carcinomas. *Cancer Cell* **2007**;12:215-29
42. Gao YF, Wang ZB, Zhu T, Mao CX, Mao XY, Li L, Yin JY, Zhou HH, Liu ZQ. A critical overview of long non-coding RNA in glioma etiology 2016: an update. *Tumour Biol* **2016**;37:14403-13
43. St Laurent G, Wahlestedt C, Kapranov P. The Landscape of long noncoding RNA classification. *Trends Genet* **2015**;31:239-51
44. Gutschner T, Diederichs S. The hallmarks of cancer: a long non-coding RNA point of view. *RNA Biol* **2012**;9:703-19
45. Brunner AL, Beck AH, Edris B, Sweeney RT, Zhu SX, Li R, Montgomery K, Varma S, Gilks T, Guo X, Foley JW, Witten DM, Giacomini CP, Flynn RA, Pollack JR, Tibshirani R, Chang HY, van de Rijn M, West RB. Transcriptional profiling of long non-coding RNAs and novel transcribed regions across a diverse panel of archived human cancers. *Genome Biol* **2012**;13:R75
46. Quek XC, Thomson DW, Maag JL, Bartonicek N, Signal B, Clark MB, Gloss BS, Dinger ME. lncRNADB v2.0: expanding the reference database for functional long noncoding RNAs. *Nucleic Acids Res* **2015**;43:D168-73
47. Quinn JJ, Chang HY. Unique features of long non-coding RNA biogenesis and function. *Nat Rev Genet* **2016**;17:47-62
48. Aguilo F, Zhou MM, Walsh MJ. Long noncoding RNA, polycomb, and the ghosts haunting INK4b-ARF-INK4a expression. *Cancer Res* **2011**;71:5365-9
49. Kotake Y, Nakagawa T, Kitagawa K, Suzuki S, Liu N, Kitagawa M, Xiong Y. Long non-coding RNA ANRIL is required for the PRC2 recruitment to and silencing of p15(INK4B) tumor suppressor gene. *Oncogene* **2011**;30:1956-62
50. Lee JT. Epigenetic regulation by long noncoding RNAs. *Science* **2012**;338:1435-9
51. Schaukowitch K, Kim TK. Emerging epigenetic mechanisms of long non-coding RNAs. *Neuroscience* **2014**;264:25-38
52. Davis CD, Uthus EO. DNA methylation, cancer susceptibility, and nutrient interactions. *Exp Biol Med (Maywood)* **2004**;229:988-95
53. Jones PA. DNA methylation errors and cancer. *Cancer Res* **1996**;56:2463-7
54. Laird PW, Jaenisch R. DNA methylation and cancer. *Hum Mol Genet* **1994**;3 Spec No:1487-95

55. Liu L, Wylie RC, Andrews LG, Tollefsbol TO. Aging, cancer and nutrition: the DNA methylation connection. *Mech Ageing Dev* **2003**;124:989-98
56. Bao X, Wu H, Zhu X, Guo X, Hutchins AP, Luo Z, Song H, Chen Y, Lai K, Yin M, Xu L, Zhou L, Chen J, Wang D, Qin B, Frampton J, Tse HF, Pei D, Wang H, Zhang B, Esteban MA. The p53-induced lincRNA-p21 derails somatic cell reprogramming by sustaining H3K9me3 and CpG methylation at pluripotency gene promoters. *Cell Res* **2015**;25:80-92
57. Ling H, Spizzo R, Atlasi Y, Nicoloso M, Shimizu M, Redis RS, Nishida N, Gafa R, Song J, Guo Z, Ivan C, Barbarotto E, De Vries I, Zhang X, Ferracin M, Churchman M, van Galen JF, Beverloo BH, Shariati M, Haderk F, Estecio MR, Garcia-Manero G, Patijn GA, Gotley DC, Bhardwaj V, Shureiqi I, Sen S, Multani AS, Welsh J, Yamamoto K, Taniguchi I, Song MA, Gallinger S, Casey G, Thibodeau SN, Le Marchand L, Tiirikainen M, Mani SA, Zhang W, Davuluri RV, Mimori K, Mori M, Sieuwerts AM, Martens JW, Tomlinson I, Negrini M, Berindan-Neagoe I, Foekens JA, Hamilton SR, Lanza G, Kopetz S, Fodde R, Calin GA. CCAT2, a novel noncoding RNA mapping to 8q24, underlies metastatic progression and chromosomal instability in colon cancer. *Genome Res* **2013**;23:1446-61
58. Takayama K, Horie-Inoue K, Katayama S, Suzuki T, Tsutsumi S, Ikeda K, Urano T, Fujimura T, Takagi K, Takahashi S, Homma Y, Ouchi Y, Aburatani H, Hayashizaki Y, Inoue S. Androgen-responsive long noncoding RNA CTBP1-AS promotes prostate cancer. *EMBO J* **2013**;32:1665-80
59. Wang G, Lunardi A, Zhang J, Chen Z, Ala U, Webster KA, Tay Y, Gonzalez-Billalabeitia E, Egia A, Shaffer DR, Carver B, Liu XS, Taulli R, Kuo WP, Nardella C, Signoretti S, Cordon-Cardo C, Gerald WL, Pandolfi PP. Zbtb7a suppresses prostate cancer through repression of a Sox9-dependent pathway for cellular senescence bypass and tumor invasion. *Nat Genet* **2013**;45:739-46
60. Flynn RA, Chang HY. Long noncoding RNAs in cell-fate programming and reprogramming. *Cell Stem Cell* **2014**;14:752-61
61. Hu W, Alvarez-Dominguez JR, Lodish HF. Regulation of mammalian cell differentiation by long non-coding RNAs. *EMBO Rep* **2012**;13:971-83
62. Rossi MN, Antonangeli F. LncRNAs: New Players in Apoptosis Control. *Int J Cell Biol* **2014**;2014:473857
63. Sutherland EW, Rall TW. Fractionation and characterization of a cyclic adenine ribonucleotide formed by tissue particles. *J Biol Chem* **1958**;232:1077-91
64. Piazza GA, Thompson WJ, Pamukcu R, Alila HW, Whitehead CM, Liu L, Fetter JR, Gresh WE, Jr., Klein-Szanto AJ, Farnell DR, Eto I, Grubbs CJ. Exisulind, a novel proapoptotic drug, inhibits rat urinary bladder tumorigenesis. *Cancer Res* **2001**;61:3961-8
65. Richter W. 3',5' Cyclic nucleotide phosphodiesterases class III: members, structure, and catalytic mechanism. *Proteins* **2002**;46:278-86
66. Francis SH, Blount MA, Corbin JD. Mammalian cyclic nucleotide phosphodiesterases: molecular mechanisms and physiological functions. *Physiol Rev* **2011**;91:651-90

67. Francis SH, Turko IV, Corbin JD. Cyclic nucleotide phosphodiesterases: relating structure and function. *Prog Nucleic Acid Res Mol Biol* **2001**;65:1-52
68. Mehats C, Andersen CB, Filopanti M, Jin SL, Conti M. Cyclic nucleotide phosphodiesterases and their role in endocrine cell signaling. *Trends Endocrinol Metab* **2002**;13:29-35
69. Callahan SM, Cornell NW, Dunlap PV. Purification and properties of periplasmic 3':5'-cyclic nucleotide phosphodiesterase. A novel zinc-containing enzyme from the marine symbiotic bacterium *Vibrio fischeri*. *J Biol Chem* **1995**;270:17627-32
70. Kimura Y, Yoshimi M, Takata G. Enzymatic and mutational analyses of a class II 3',5'-cyclic nucleotide phosphodiesterase, PdeE, from *Myxococcus xanthus*. *J Bacteriol* **2011**;193:2053-7
71. Powell S, Forslund K, Szklarczyk D, Trachana K, Roth A, Huerta-Cepas J, Gabaldon T, Rattei T, Creevey C, Kuhn M, Jensen LJ, von Mering C, Bork P. eggNOG v4.0: nested orthology inference across 3686 organisms. *Nucleic Acids Res* **2014**;42:D231-9
72. Fuchs EL, Brutinel ED, Klem ER, Fehr AR, Yahr TL, Wolfgang MC. In vitro and in vivo characterization of the *Pseudomonas aeruginosa* cyclic AMP (cAMP) phosphodiesterase CpdA, required for cAMP homeostasis and virulence factor regulation. *J Bacteriol* **2010**;192:2779-90
73. Imamura R, Yamanaka K, Ogura T, Hiraga S, Fujita N, Ishihama A, Niki H. Identification of the cpdA gene encoding cyclic 3',5'-adenosine monophosphate phosphodiesterase in *Escherichia coli*. *J Biol Chem* **1996**;271:25423-9
74. Kimura Y, Okazaki N, Takegawa K. Enzymatic characteristics of two novel *Myxococcus xanthus* enzymes, PdeA and PdeB, displaying 3',5'- and 2',3'-cAMP phosphodiesterase, and phosphatase activities. *FEBS Lett* **2009**;583:443-8
75. Mathieu-Demaziere C, Poinot V, Masson-Boivin C, Garnerone AM, Batut J. Biochemical and functional characterization of SpdA, a 2', 3'cyclic nucleotide phosphodiesterase from *Sinorhizobium meliloti*. *BMC Microbiol* **2013**;13:268
76. Podobnik M, Tyagi R, Matange N, Dermol U, Gupta AK, Mattoo R, Seshadri K, Visweswariah SS. A mycobacterial cyclic AMP phosphodiesterase that moonlights as a modifier of cell wall permeability. *J Biol Chem* **2009**;284:32846-57
77. Shenoy AR, Capuder M, Draskovic P, Lamba D, Visweswariah SS, Podobnik M. Structural and biochemical analysis of the Rv0805 cyclic nucleotide phosphodiesterase from *Mycobacterium tuberculosis*. *J Mol Biol* **2007**;365:211-25
78. Matange N, Podobnik M, Visweswariah SS. Metallophosphoesterases: structural fidelity with functional promiscuity. *Biochem J* **2015**;467:201-16
79. Matange N. Revisiting bacterial cyclic nucleotide phosphodiesterases: cyclic AMP hydrolysis and beyond. *FEMS Microbiol Lett* **2015**;362
80. Connelly JC, Leach DR. Tethering on the brink: the evolutionarily conserved Mre11-Rad50 complex. *Trends Biochem Sci* **2002**;27:410-8
81. Ren J, Mi Z, Stewart NA, Jackson EK. Identification and quantification of 2',3'-cAMP release by the kidney. *J Pharmacol Exp Ther* **2009**;328:855-65

82. Levy I, Horvath A, Azevedo M, de Alexandre RB, Stratakis CA. Phosphodiesterase function and endocrine cells: links to human disease and roles in tumor development and treatment. *Curr Opin Pharmacol* **2011**;11:689-97
83. Maurice DH, Ke H, Ahmad F, Wang Y, Chung J, Manganiello VC. Advances in targeting cyclic nucleotide phosphodiesterases. *Nat Rev Drug Discov* **2014**;13:290-314
84. Hirsh L, Dantes A, Suh BS, Yoshida Y, Hosokawa K, Tajima K, Kotsuji F, Merimsky O, Amsterdam A. Phosphodiesterase inhibitors as anti-cancer drugs. *Biochem Pharmacol* **2004**;68:981-8
85. Zhang DD, Li Y, Xu Y, Kim J, Huang S. Phosphodiesterase 7B/microRNA-200c relationship regulates triple-negative breast cancer cell growth. *Oncogene* **2019**;38:1106-20
86. Whitehead CM, Earle KA, Fetter J, Xu S, Hartman T, Chan DC, Zhao TL, Piazza G, Klein-Szanto AJ, Pamukcu R, Alila H, Bunn PA, Jr., Thompson WJ. Exisulind-induced apoptosis in a non-small cell lung cancer orthotopic lung tumor model augments docetaxel treatment and contributes to increased survival. *Mol Cancer Ther* **2003**;2:479-88
87. Zhang L, Murray F, Rassenti LZ, Pu M, Kelly C, Kanter JR, Greaves A, Messer K, Kipps TJ, Insel PA. Cyclic nucleotide phosphodiesterase 7B mRNA: an unfavorable characteristic in chronic lymphocytic leukemia. *Int J Cancer* **2011**;129:1162-9
88. Zhang L, Murray F, Zahno A, Kanter JR, Chou D, Suda R, Fenlon M, Rassenti L, Cottam H, Kipps TJ, Insel PA. Cyclic nucleotide phosphodiesterase profiling reveals increased expression of phosphodiesterase 7B in chronic lymphocytic leukemia. *Proc Natl Acad Sci U S A* **2008**;105:19532-7
89. Li N, Lee K, Xi Y, Zhu B, Gary BD, Ramirez-Alcantara V, Gurpinar E, Canzoneri JC, Fajardo A, Sigler S, Piazza JT, Chen X, Andrews J, Thomas M, Lu W, Li Y, Laan DJ, Moyer MP, Russo S, Eberhardt BT, Yet L, Keeton AB, Grizzle WE, Piazza GA. Phosphodiesterase 10A: a novel target for selective inhibition of colon tumor cell growth and beta-catenin-dependent TCF transcriptional activity. *Oncogene* **2015**;34:1499-509
90. Ahn YH, Jung JM, Hong SH. 8-Chloro-cyclic AMP-induced growth inhibition and apoptosis is mediated by p38 mitogen-activated protein kinase activation in HL60 cells. *Cancer Res* **2005**;65:4896-901
91. Tortora G, Ciardiello F. Protein kinase A as target for novel integrated strategies of cancer therapy. *Ann N Y Acad Sci* **2002**;968:139-47
92. Wang HM, Zheng NG, Wu JL, Gong CC, Wang YL. Dual effects of 8-Br-cAMP on differentiation and apoptosis of human esophageal cancer cell line Eca-109. *World J Gastroenterol* **2005**;11:6538-42
93. Cho-Chung YS, Nesterova MV. Tumor reversion: protein kinase A isozyme switching. *Ann N Y Acad Sci* **2005**;1058:76-86
94. Drees M, Zimmermann R, Eisenbrand G. 3',5'-Cyclic nucleotide phosphodiesterase in tumor cells as potential target for tumor growth inhibition. *Cancer Res* **1993**;53:3058-61

95. Savai R, Pullamsetti SS, Banat GA, Weissmann N, Ghofrani HA, Grimminger F, Schermuly RT. Targeting cancer with phosphodiesterase inhibitors. *Expert Opin Investig Drugs* **2010**;19:117-31
96. Page CP, Spina D. Phosphodiesterase inhibitors in the treatment of inflammatory diseases. *Handb Exp Pharmacol* **2011**:391-414
97. Bjorgo E, Moltu K, Tasken K. Phosphodiesterases as targets for modulating T-cell responses. *Handb Exp Pharmacol* **2011**:345-63
98. Hertz AL, Beavo JA. Cyclic nucleotides and phosphodiesterases in monocytic differentiation. *Handb Exp Pharmacol* **2011**:365-90
99. Das A, Durrant D, Mitchell C, Mayton E, Hoke NN, Salloum FN, Park MA, Qureshi I, Lee R, Dent P, Kukreja RC. Sildenafil increases chemotherapeutic efficacy of doxorubicin in prostate cancer and ameliorates cardiac dysfunction. *Proc Natl Acad Sci U S A* **2010**;107:18202-7
100. Tyagi R, Shenoy AR, Visweswariah SS. Characterization of an evolutionarily conserved metallophosphoesterase that is expressed in the fetal brain and associated with the WAGR syndrome. *J Biol Chem* **2009**;284:5217-28
101. Schwartz F, Eisenman R, Knoll J, Gessler M, Bruns G. cDNA sequence, genomic organization, and evolutionary conservation of a novel gene from the WAGR region. *Genomics* **1995**;29:526-32
102. Schwartz F, Neve R, Eisenman R, Gessler M, Bruns G. A WAGR region gene between PAX-6 and FSHB expressed in fetal brain. *Hum Genet* **1994**;94:658-64
103. Dermal U, Janardan V, Tyagi R, Visweswariah SS, Podobnik M. Unique utilization of a phosphoprotein phosphatase fold by a mammalian phosphodiesterase associated with WAGR syndrome. *J Mol Biol* **2011**;412:481-94
104. Swarbrick JD, Shaw DJ, Chhabra S, Ghai R, Valkov E, Norwood SJ, Seaman MN, Collins BM. VPS29 is not an active metallo-phosphatase but is a rigid scaffold required for retromer interaction with accessory proteins. *PLoS One* **2011**;6:e20420
105. Liguori L, Andolfo I, de Antonellis P, Aglio V, di Dato V, Marino N, Orloff NI, De Martino D, Capasso M, Petrosino G, Schramm A, Navas L, Tonini GP, Eggert A, Iolascon A, Zollo M. The metallophosphodiesterase Mpped2 impairs tumorigenesis in neuroblastoma. *Cell Cycle* **2012**;11:569-81
106. Zhang R, Shen C, Zhao L, Wang J, McCrae M, Chen X, Lu F. Dysregulation of host cellular genes targeted by human papillomavirus (HPV) integration contributes to HPV-related cervical carcinogenesis. *Int J Cancer* **2016**;138:1163-74
107. Shen L, Liu L, Ge L, Xie L, Liu S, Sang L, Zhan T, Li H. miR-448 downregulates MPPED2 to promote cancer proliferation and inhibit apoptosis in oral squamous cell carcinoma. *Exp Ther Med* **2016**;12:2747-52
108. Gu S, Lin S, Ye D, Qian S, Jiang D, Zhang X, Li Q, Yang J, Ying X, Li Z, Tang M, Wang J, Jin M, Chen K. Genome-wide methylation profiling identified novel differentially hypermethylated biomarker MPPED2 in colorectal cancer. *Clin Epigenetics* **2019**;11:41

109. Fagin JA, Wells SA, Jr. Biologic and Clinical Perspectives on Thyroid Cancer. *N Engl J Med* **2016**;375:2307
110. Nikiforov YE. Molecular diagnostics of thyroid tumors. *Arch Pathol Lab Med* **2011**;135:569-77
111. Saji M, Ringel MD. The PI3K-Akt-mTOR pathway in initiation and progression of thyroid tumors. *Mol Cell Endocrinol* **2010**;321:20-8
112. Xing M. Genetic alterations in the phosphatidylinositol-3 kinase/Akt pathway in thyroid cancer. *Thyroid* **2010**;20:697-706
113. Dwight T, Thoppe SR, Foukakis T, Lui WO, Wallin G, Hoog A, Frisk T, Larsson C, Zedenius J. Involvement of the PAX8/peroxisome proliferator-activated receptor gamma rearrangement in follicular thyroid tumors. *J Clin Endocrinol Metab* **2003**;88:4440-5
114. Nikiforova MN, Lynch RA, Biddinger PW, Alexander EK, Dorn GW, 2nd, Tallini G, Kroll TG, Nikiforov YE. RAS point mutations and PAX8-PPAR gamma rearrangement in thyroid tumors: evidence for distinct molecular pathways in thyroid follicular carcinoma. *J Clin Endocrinol Metab* **2003**;88:2318-26
115. Nikiforova MN, Nikiforov YE. Molecular diagnostics and predictors in thyroid cancer. *Thyroid* **2009**;19:1351-61
116. Vasko V, Ferrand M, Di Cristofaro J, Carayon P, Henry JF, de Micco C. Specific pattern of RAS oncogene mutations in follicular thyroid tumors. *J Clin Endocrinol Metab* **2003**;88:2745-52
117. Xing M. BRAF mutation in papillary thyroid cancer: pathogenic role, molecular bases, and clinical implications. *Endocr Rev* **2007**;28:742-62
118. Kunstman JW, Juhlin CC, Goh G, Brown TC, Stenman A, Healy JM, Rubinstein JC, Choi M, Kiss N, Nelson-Williams C, Mane S, Rimm DL, Prasad ML, Hoog A, Zedenius J, Larsson C, Korah R, Lifton RP, Carling T. Characterization of the mutational landscape of anaplastic thyroid cancer via whole-exome sequencing. *Hum Mol Genet* **2015**;24:2318-29
119. Xing M, Clark D, Guan H, Ji M, Dackiw A, Carson KA, Kim M, Tufaro A, Ladenson P, Zeiger M, Tufano R. BRAF mutation testing of thyroid fine-needle aspiration biopsy specimens for preoperative risk stratification in papillary thyroid cancer. *J Clin Oncol* **2009**;27:2977-82
120. Di Cristofaro J, Marcy M, Vasko V, Sebag F, Fakhry N, Wynford-Thomas D, De Micco C. Molecular genetic study comparing follicular variant versus classic papillary thyroid carcinomas: association of N-ras mutation in codon 61 with follicular variant. *Hum Pathol* **2006**;37:824-30
121. Esapa CT, Johnson SJ, Kendall-Taylor P, Lennard TW, Harris PE. Prevalence of Ras mutations in thyroid neoplasia. *Clin Endocrinol (Oxf)* **1999**;50:529-35
122. Kondo T, Ezzat S, Asa SL. Pathogenetic mechanisms in thyroid follicular-cell neoplasia. *Nat Rev Cancer* **2006**;6:292-306
123. Santarpia L, Myers JN, Sherman SI, Trimarchi F, Clayman GL, El-Naggar AK. Genetic alterations in the RAS/RAF/mitogen-activated protein kinase and

- phosphatidylinositol 3-kinase/Akt signaling pathways in the follicular variant of papillary thyroid carcinoma. *Cancer* **2010**;116:2974-83
124. Ellis MJ, Gillette M, Carr SA, Paulovich AG, Smith RD, Rodland KK, Townsend RR, Kinsinger C, Mesri M, Rodriguez H, Liebler DC, Clinical Proteomic Tumor Analysis C. Connecting genomic alterations to cancer biology with proteomics: the NCI Clinical Proteomic Tumor Analysis Consortium. *Cancer Discov* **2013**;3:1108-12
125. Vogelstein B, Kinzler KW. Has the breast cancer gene been found? *Cell* **1994**;79:1-3
126. Deroo BJ, Korach KS. Estrogen receptors and human disease. *J Clin Invest* **2006**;116:561-70
127. Gao X, Nawaz Z. Progesterone receptors - animal models and cell signaling in breast cancer: Role of steroid receptor coactivators and corepressors of progesterone receptors in breast cancer. *Breast Cancer Res* **2002**;4:182-6
128. Hynes NE, Stern DF. The biology of erbB-2/neu/HER-2 and its role in cancer. *Biochim Biophys Acta* **1994**;1198:165-84
129. Miecznikowski JC, Wang D, Liu S, Sucheston L, Gold D. Comparative survival analysis of breast cancer microarray studies identifies important prognostic genetic pathways. *BMC Cancer* **2010**;10:573
130. Blows FM, Driver KE, Schmidt MK, Broeks A, van Leeuwen FE, Wesseling J, Cheang MC, Gelmon K, Nielsen TO, Blomqvist C, Heikkila P, Heikkinen T, Nevanlinna H, Akslen LA, Begin LR, Foulkes WD, Couch FJ, Wang X, Cafourek V, Olson JE, Baglietto L, Giles GG, Severi G, McLean CA, Southey MC, Rakha E, Green AR, Ellis IO, Sherman ME, Lissowska J, Anderson WF, Cox A, Cross SS, Reed MW, Provenzano E, Dawson SJ, Dunning AM, Humphreys M, Easton DF, Garcia-Closas M, Caldas C, Pharoah PD, Huntsman D. Subtyping of breast cancer by immunohistochemistry to investigate a relationship between subtype and short and long term survival: a collaborative analysis of data for 10,159 cases from 12 studies. *PLoS Med* **2010**;7:e1000279
131. Vallejos CS, Gomez HL, Cruz WR, Pinto JA, Dyer RR, Velarde R, Suazo JF, Neciosup SP, Leon M, de la Cruz MA, Vigil CE. Breast cancer classification according to immunohistochemistry markers: subtypes and association with clinicopathologic variables in a peruvian hospital database. *Clin Breast Cancer* **2010**;10:294-300
132. Kondov B, Milenkovic Z, Kondov G, Petrushevska G, Basheska N, Bogdanovska-Todorovska M, Tolevska N, Ivkovski L. Presentation of the Molecular Subtypes of Breast Cancer Detected By Immunohistochemistry in Surgically Treated Patients. *Open Access Maced J Med Sci* **2018**;6:961-7
133. Cianfrocca M, Gradishar W. New molecular classifications of breast cancer. *CA Cancer J Clin* **2009**;59:303-13
134. Diez-Villanueva A, Mallona I, Peinado MA. Wanderer, an interactive viewer to explore DNA methylation and gene expression data in human cancer. *Epigenetics Chromatin* **2015**;8:22

135. Yap KL, Li S, Munoz-Cabello AM, Raguz S, Zeng L, Mujtaba S, Gil J, Walsh MJ, Zhou MM. Molecular interplay of the noncoding RNA ANRIL and methylated histone H3 lysine 27 by polycomb CBX7 in transcriptional silencing of INK4a. *Mol Cell* **2010**;38:662-74
136. Di Ruscio A, Ebralidze AK, Benoukraf T, Amabile G, Goff LA, Terragni J, Figueroa ME, De Figueiredo Pontes LL, Alberich-Jorda M, Zhang P, Wu M, D'Alo F, Melnick A, Leone G, Ebralidze KK, Pradhan S, Rinn JL, Tenen DG. DNMT1-interacting RNAs block gene-specific DNA methylation. *Nature* **2013**;503:371-6
137. Merry CR, Forrest ME, Sabers JN, Beard L, Gao XH, Hatzoglou M, Jackson MW, Wang Z, Markowitz SD, Khalil AM. DNMT1-associated long non-coding RNAs regulate global gene expression and DNA methylation in colon cancer. *Hum Mol Genet* **2015**;24:6240-53
138. Bernardino J, Roux C, Almeida A, Vogt N, Gibaud A, Gerbault-Seureau M, Magdelenat H, Bourgeois CA, Malfoy B, Dutrillaux B. DNA hypomethylation in breast cancer: an independent parameter of tumor progression? *Cancer Genet Cytogenet* **1997**;97:83-9
139. Jair KW, Bachman KE, Suzuki H, Ting AH, Rhee I, Yen RW, Baylin SB, Schuebel KE. De novo CpG island methylation in human cancer cells. *Cancer Res* **2006**;66:682-92
140. Lin RK, Hsu HS, Chang JW, Chen CY, Chen JT, Wang YC. Alteration of DNA methyltransferases contributes to 5'CpG methylation and poor prognosis in lung cancer. *Lung Cancer* **2007**;55:205-13
141. Pathania R, Ramachandran S, Elangovan S, Padia R, Yang P, Cinghu S, Veeranan-Karmegam R, Arjunan P, Gnana-Prakasam JP, Sadanand F, Pei L, Chang CS, Choi JH, Shi H, Manicassamy S, Prasad PD, Sharma S, Ganapathy V, Jothi R, Thangaraju M. DNMT1 is essential for mammary and cancer stem cell maintenance and tumorigenesis. *Nat Commun* **2015**;6:6910
142. Soares J, Pinto AE, Cunha CV, Andre S, Barao I, Sousa JM, Cravo M. Global DNA hypomethylation in breast carcinoma: correlation with prognostic factors and tumor progression. *Cancer* **1999**;85:112-8
143. Eger A, Aigner K, Sonderegger S, Dampier B, Oehler S, Schreiber M, Berx G, Cano A, Beug H, Foisner R. DeltaEF1 is a transcriptional repressor of E-cadherin and regulates epithelial plasticity in breast cancer cells. *Oncogene* **2005**;24:2375-85
144. Oka H, Shiozaki H, Kobayashi K, Inoue M, Tahara H, Kobayashi T, Takatsuka Y, Matsuyoshi N, Hirano S, Takeichi M, et al. Expression of E-cadherin cell adhesion molecules in human breast cancer tissues and its relationship to metastasis. *Cancer Res* **1993**;53:1696-701
145. Schmalhofer O, Brabletz S, Brabletz T. E-cadherin, beta-catenin, and ZEB1 in malignant progression of cancer. *Cancer Metastasis Rev* **2009**;28:151-66
146. Wu H, Zhang Y. Reversing DNA methylation: mechanisms, genomics, and biological functions. *Cell* **2014**;156:45-68
147. Hansen KD, Timp W, Bravo HC, Sabunciyan S, Langmead B, McDonald OG, Wen B, Wu H, Liu Y, Diep D, Briem E, Zhang K, Irizarry RA, Feinberg AP.

Increased methylation variation in epigenetic domains across cancer types. *Nat Genet* **2011**;43:768-75

148. Qi D, Li J, Que B, Su J, Li M, Zhang C, Yang M, Zhou G, Ji W. Long non-coding RNA DBCCR1-003 regulate the expression of DBCCR1 via DNMT1 in bladder cancer. *Cancer Cell Int* **2016**;16:81